Feasibility of using rural waste products to increase the denitrification efficiency in a surface flow constructed wetland.

Rosanna Margalef-Marti, Raúl Carrey, Daniel Merchán, Albert Soler, Jesús Causapé, Neus Otero

Journal of Hydrology, 2019, Volume 578, 124035
DOI: https://doi.org/10.1016/j.jhydrol.2019.124035

Received date: 23 April 2019
Revised date: 7 August 2019
Accepted date: 9 August 2019
Available online: 13 August 2019

Feasibility of using rural waste products to increase the denitrification efficiency in a surface flow constructed wetland

Rosanna Margalef-Marti[1], Raúl Carrey[1], Daniel Merchán[2], Albert Soler[1], Jesús Causapé[3], Neus Otero[1,4]

[1] Grup MAiMA, SGR Mineralogia Aplicada, Geoquímica i Geomicrobiologia, Departament de Mineralogia, Petrologia i Geologia Aplicada, SIMGEO UB-CSIC, Facultat de Ciències de la Terra, Universitat de Barcelona (UB), C/Martí i Franquès s/n, 08028, Barcelona, Spain

[2] Department of Engineering, IS-FOOD Institute (Innovation & Sustainable Development in Food Chain), Public University of Navarre, Campus de Arrosadia, 31006, Pamplona, Navarra, Spain

[3] Geological Survey of Spain—IGME, C/Manuel Lasala 44 9◦B, 50006, Zaragoza, Spain

[4] Serra Húnter Fellowship, Generalitat de Catalunya, Spain.

ABSTRACT

A surface flow constructed wetland (CW) was set in the Lerma gully to decrease nitrate (NO_3^-) pollution from agricultural runoff water. The water flow rate and NO_3^- concentration were monitored at the inlet and the outlet, and sampling campaigns were performed which consisted of collecting six water samples along the CW flow line. After two years of operation, the NO_3^- attenuation was limited at a flow rate of ~2.5 L/s and became negligible at ~5.5 L/s. The present work aimed to assess the feasibility of using rural waste products (wheat hay, corn stubble, and animal compost) to induce denitrification in the CW, to assess the effect of temperature on this process, and to trace the efficiency of the treatment by using isotopic tools. In the first stage, microcosm experiments were performed. Afterwards, the selected waste material was applied in the CW, and the treatment efficiency was evaluated by means of a chemical and isotopic characterization and using the isotopic fractionation (ε) values calculated from laboratory experiments to avoid field-scale interference. The microcosms results showed that the stubble was the most appropriate material for application in the CW, but the denitrification rate was found to decrease with temperature. In the CW, biostimulation in autumn-winter promoted NO_3^- attenuation between two weeks and one month (a reduction in NO_3^- between 1.2 and 1.5 mM

was achieved). After the biostimulation in spring-summer, the attenuation was maintained for approximately three months (NO_3^- reduction between 0.1 and 1.5 mM). The $\varepsilon^{15}N_{NO3/N2}$ and $\varepsilon^{18}O_{NO3/N2}$ values obtained from the laboratory experiments allowed to estimate the induced denitrification percentage. At an approximate average flow rate of 16 L/s, at least 60 % of NO_3^- attenuation was achieved in the CW. The field samples exhibited a slope of 1.0 for $\delta^{18}O\text{-}NO_3^-$ versus $\delta^{15}N\text{-}NO_3^-$, similar to those of the laboratory experiments (0.9-1.2). Plant uptake seemed to play a minor role in NO_3^- attenuation in the CW. Hence, the application of stubble in the CW allowed the removal of large amounts of NO_3^- from the Lerma gully, especially when applied during the warm months, but its efficacy was limited to a short time period (up to three months).

Keywords: denitrification, constructed wetland, electron donor, isotopic fractionation, remediation.

1. INTRODUCTION

Since nitrate (NO_3^-) is known to cause ecological and human health problems (Vitousek et al., 1997; Ward et al., 2005), the presence of this nutrient in water bodies worldwide is a matter of concern. The extensive application of synthetic and organic fertilizers is a major source of NO_3^- pollution. Therefore, agricultural runoff water should be treated before it is drained into larger water bodies such as aquifers, rivers, and/or lakes. Constructed wetlands (CWs) are considered promising, low cost systems for the remediation of diverse water pollutants, are simple to operate, and have low energy requirements (Wu et al., 2015). Hence, directing agricultural runoff water through a CW could be useful for removing NO_3^- to minimize pollution.

The surface flow CWs consists of free surface water flowing horizontally through an artificial pond containing floating and/or emergent rooted vegetation and a high diversity of microorganisms (Ilyas and Masih, 2017; Sirivedhin and Gray, 2006; Vymazal, 2007). The main processes that might contribute to NO_3^- pollution mitigation in surface flow CWs are plant uptake, assimilation by microorganisms, and denitrification (Rogers et al., 1991). The latter refers to the reduction of NO_3^- by microorganisms through a series of enzymatic reactions involving the intermediates NO_2^-, NO, and N_2O, before finally being reduced to N_2 (Knowles, 1982). Parameters such as temperature, dissolved oxygen (O_2), NO_3^- loading, the source and amount of organic carbon (C), microbial species, the type and density of macrophytes, wetland age, and hydraulic conditions play key

roles in the NO_3^- removal efficiency (Bachand and Horne, 1999; Beutel et al., 2009; Kong et al., 2009; Sirivedhin and Gray, 2006). Different approaches can be implemented to enhance water remediation, but strategies directed toward the induction of bacterial NO_3^- respiration are preferred since denitrification is an authentic N sink in water, unlike biomass sequestration (Scott et al., 2008). N storage by plants is generally considered temporary, because organic N returns to the system after the death and decay of plants if they are not harvested (Cooper and Cooke, 1984; Gumbricht, 1993).

In CWs, macrophytes are able not only to assimilate NO_3^-, but also to promote denitrification efficiency. Plants exert an influence on the diversity of microbial species and their enzymatic activities by releasing exudates and oxygen to the rhizosphere (Kong et al., 2009, and references therein), and decomposed plant material can be used by microbes as a source of organic C. For this reason, increased NO_3^- removal is usually found in vegetated CWs relative to that in non-vegetated systems (Jacobs and Harrison, 2014; Soana et al., 2017). If the CW cannot provide enough organic C to support complete denitrification (e.g., from inlet water, soil, plant root exudates, and decomposed vegetal material), the addition of an external organic C source as an electron donor could enhance the heterotrophic denitrification efficiency (Lu et al., 2009; Si et al., 2018). Since the use of pure reagents such as glucose, acetate, or ethanol may be expensive in long-term treatments, the use of industrial or agricultural residues that are rich in organic C could represent a more sustainable solution. Solid products such as animal or vegetal waste (Grau-Martínez et al., 2017; Si et al., 2018; Trois et al., 2010), as well as industrial liquid by-products (Carrey et al., 2018; Margalef-Marti et al., 2019), have already been reported as being useful for promoting denitrification.

The pollutant removal efficiency in CWs can be estimated by monitoring the inlet and outlet concentrations of the pollutant (Kovacic et al., 2000; Tanner et al., 2005; Uusheimo et al., 2018). However, this method does not reveal the specific processes involved in the attenuation, making it challenging to focus on the improvement of the wetland design and operation. Stable isotope analyses can provide information on the NO_3^- transformation pathways. In the course of denitrification, the unreacted residual NO_3^- becomes enriched in the heavy isotopes ^{15}N and ^{18}O, permitting the distinction between biological attenuation and other processes such as dilution which could also lead to decreases in concentration without influencing the isotopic signature

(Böttcher et al., 1990; Fukada et al., 2003; Mariotti et al., 1981; Aravena and Robertson, 1998). In plants, significant enrichment in both ^{15}N and ^{18}O is observed in the NO_3^- extracted from leaves after uptake relative to the NO_3^- from water, but the changes in the NO_3^- isotopic composition in the water are minor (Estrada et al., 2017; Spoelstra et al., 2010). Therefore, the NO_3^- isotopic characterization of water samples collected at the CW might improve the understanding and support the evaluation of the performance of the remediation strategy.

In this context, the present work was developed to assess the feasibility of using rural waste products (wheat hay, corn stubble, and animal compost) to induce denitrification in a surface flow CW, and to trace the treatment efficiency in the autumn-winter and spring-summer seasons. In the first stage, lab-scale experiments were performed to identify the most appropriate electron donor to be applied in the CW, and to evaluate the effect of temperature on NO_3^- reduction. The isotopic fractionations (ε) of N and O of dissolved NO_3^- under each condition were also determined. In the second stage, the selected material was applied in the CW and the treatment efficiency was evaluated by means of a chemical and isotopic characterization using the ε values calculated from the laboratory experiments.

2. METHODS

2.1. Laboratory experiments

Six types of batch experiments were performed in 150 mL crystal Pyrex® bottles crimp-sealed with butyl rubber stoppers under an argon (Ar) headspace. Each microcosm contained 100 mL of water (2 mM NO_3^-) collected from the inlet of the studied CW (see Section 2.2) and a specific C source: corn stubble (1 g); wheat hay (1 g); or animal compost (0.25 g). The six series of parallel experiments were determined according to the waste product employed and the incubation temperature. Series I (C-24) and II (H-24) contained animal compost and wheat hay, respectively, and were incubated at 24 ºC; series III (S-24), IV (S-16), and V (S-8) contained corn stubble and were incubated at 24 ºC, 16 ºC, and 8 ºC, respectively; series VI (DS-24) contained partially decomposed corn stubble and was incubated at 24 ºC. The partially decomposed stubble was obtained from the CW 7.5 months after its application on September 25, 2017 (see Section 2.2). All series included at least eight replicates of the biostimulated microcosms. Control microcosms for each tested material were prepared using deionized water (DIW) to discard the potential

supply of N from the waste products. The detailed content of each microcosm is described in **Table 1**. During incubation, all microcosms were maintained in darkness and under constant vibratory shaking. The biostimulated microcosms were sacrificed at time intervals depending on the denitrification dynamics until complete NO_3^- and NO_2^- removals were achieved. The control microcosms were sacrificed at the end of the biostimulation experiments. Water samples from batch experiments were analyzed for major anions (NO_3^-, NO_2^-, Cl^-, and SO_4^{2-}), ammonium (NH_4^+), non-purgeable dissolved organic C (NPDOC), dissolved inorganic C (DIC), major cations, trace elements, δ^{15}N-NO_3^-, δ^{18}O-NO_3^-, and δ^{13}C-DIC. Samples from control microcosms were analyzed for major anions and NPDOC. The gas accumulated in the headspace of the vials was collected and analyzed for nitrous oxide (N_2O) concentration. The three organic C sources were analyzed for C and N concentrations and $\delta^{13}C\text{-}C_{bulk}$ and $\delta^{15}N\text{-}N_{bulk}$.

2.2. CW test

In the 2000s, approximately 20,000 ha of rainfed croplands were transformed into irrigated agricultural land in the Arba River Basin (Zaragoza, Spain). A small watershed representative of the area (Lerma basin, 733 ha) was monitored to assess the effects of this transformation on the water balance and the salt and NO_3^--N exports (Merchán et al., 2015, 2014, 2013). In general, the implementation of irrigation implied a three-fold increase in N export to the receiving water bodies, in this case the Arba River, which was the first surface water body in the Ebro River Basin to be declared affected by NO_3^- pollution according to the Nitrates Directive 91/676/EEC. In order to diminish the release of NO_3^- from the Lerma Basin to the Arba River, a surface flow CW was constructed in October 2015, initially covering an area of ~1500 m^2, and was enlarged in June 2017, covering a final area of ~2500 m^2 with a depth of ~40 cm. The surface water of the Lerma gully can be partially diverted towards the CW. Water flow in the Lerma gully varies between 15 and 60 L/s. Temperature and precipitation data collected monthly in the area are reported in Supporting information (**Table S1**).

The CW is fully automated, with high-frequency monitoring (every 10 minutes) of the water flow rate and NO_3^- concentration at both the inlet and the outlet. Emergent macrophytes (*Typha* and *Phragmites*) started growing since its construction, and occupied approximately 75 % of the CW surface at the time the present study began, since the enlarged part was still unvegetated. The

145 field survey was performed in three periods and involved 13 sampling campaigns, each consisting
146 of the collection of six water samples (H1 to H6) from along the wetland flow line (**Figure 1**). In
147 the first period (June to September 2017), two different operating conditions were tested before
148 the biostimulation by modifying the inlet opening; three sampling campaigns were performed at
149 two different flow rates (~5.5 L/s and ~2.5 L/s). The second period involved the application of corn
150 stubble obtained from the surrounding crops (~8000 kg) on September 25, 2017, and the
151 evaluation of treatment efficiency by performing two sampling campaigns 7 and 14 d after the
152 application. The third period involved a second application of corn stubble (~6000 kg) on May 11,
153 2018, and the evaluation of treatment efficiency by performing eight sampling campaigns from
154 May 2018 to October 2018. In the two biostimulation periods, the corn stubble was applied over
155 all the CW surface between H1 and H3. Throughout these second and third periods, the CW was
156 operated at a higher flow rate (~16 L/s). The given flow rate for the CW test periods is that
157 measured at the outlet. The calculated residence time of NO_3^- in the CW was 21, 51 and 112 h
158 for the tested flow rates of 16, 5.5 and 2.5 L/s, respectively. Detailed information about the
159 sampling campaigns is shown in **Table 2**. Water samples collected at the CW were analyzed for
160 major anions (NO_3^-, NO_2^-, Cl^-, and SO_4^{2-}), NH_4^+, NPDOC, DIC, major cations, trace elements,
161 $\delta^{15}N\text{-}NO_3^-$, $\delta^{18}O\text{-}NO_3^-$, $\delta^{34}S\text{-}SO_4^{2-}$, $\delta^{18}O\text{-}SO_4^{2-}$, and $\delta^{13}C$-DIC.

162 *2.3. Analytical methods*

163 Water samples for the field and laboratory batch experiments were immediately filtered through
164 0.2 µm Millipore® filters after being collected, and were stored at 4 ºC until analysis. The aliquots
165 for NH_4^+, $\delta^{15}N\text{-}NO_3^-$, and $\delta^{18}O\text{-}NO_3^-$ analysis were frozen, and the aliquots for the DIC and $\delta^{13}C$-
166 DIC analyses were left with no headspace and stored at 4 ºC.

167 Anions (Cl^-, NO_2^-, NO_3^-, and SO_4^{2-}) were analyzed by high-performance liquid chromatography
168 (HPLC) (Waters 515 pump and Waters IC-Pak anion column with Waters 432 and KONTRON
169 UV/Vis detectors). NH_4^+ was analyzed by three techniques due to equipment availability issues:
170 I) spectrophotometry using the indophenol blue method (CARY 1E UV-visible), II) ion
171 chromatography or III) ammonia ion selective electrode (ORION, Thermo Scientific). DIC was
172 analyzed by titration (METROHM 702 SM Titrino), NPDOC by organic matter combustion (TOC
173 500 SHIMADZU), and major cations and trace elements by ICP-OES (Perkin Elmer Optima 8300).

The concentration of N_2O accumulated at the headspace of the vials was analyzed by gas chromatography (GC) (Thermo Scientific Trace 1300 with ECD detector), and C and N concentrations in the waste materials employed as C sources were analyzed with an elemental analyzer (EA) (Carlo Erba1108 CHNS-O EA). The $\delta^{15}N\text{-}NO_3^-$ and $\delta^{18}O\text{-}NO_3^-$ were determined following the cadmium and azide reduction method (McIlvin and Altabet, 2005; Ryabenko et al., 2009). The isotopic composition of the N_2O obtained from the NO_3^- reduction was analyzed using a Pre-Con coupled to a Finnigan MAT 253 isotope ratio mass spectrometer (IRMS) (Thermo Scientific). For the SO_4^{2-} isotopic analysis, the dissolved SO_4^{2-} was precipitated as $BaSO_4$ by adding $BaCl_2 \cdot 2H_2O$ after acidifying the sample with HCl and boiling it in order to prevent precipitation of $BaCO_3$ (Dogramaci et al., 2001). The $\delta^{34}S\text{-}SO_4^{2-}$ was analyzed with a Carlo Erba EA coupled in continuous flow to a Finnigan Delta XP Plus IRMS, whereas the $\delta^{18}O\text{-}SO_4^{2-}$ was analyzed with a ThermoQuest high-temperature conversion analyzer (TC/EA) coupled in continuous flow to a Finnigan Matt Delta XP Plus IRMS. The $\delta^{13}C\text{-}DIC$ was analyzed via carbonate conversion to CO_2 gas by adding a phosphoric acid solution and measuring the gas evolved with a Gas-Bench II coupled to a MAT-253 IRMS (Thermo Scientific). The $\delta^{13}C\text{-}C_{bulk}$ and $\delta^{15}N\text{-}N_{bulk}$ of the waste materials employed as C sources were determined with a Carlo Erba EA coupled to a Finnigan Delta C IRMS.

The isotopic notation is expressed in terms of δ (‰) relative to the international standards: atmospheric N_2 (AIR) for $\delta^{15}N$, Vienna Standard Mean Oceanic Water (V-SMOW) for $\delta^{18}O$, Vienna Pee Dee Belemnite (V-PDB) for $\delta^{13}C$, and Vienna Canyon Diablo Troillite (V-CDT) for $\delta^{34}S$. Hence, $\delta = ((R_{sample}\text{-}R_{standard})/R_{standard})$, where R is the ratio between the heavy and the light isotopes. Following Coplen (2011), several international and laboratory (CCiT) standards were interspersed among the samples for normalization of the results (Supporting Information **Table S2**). The reproducibilities (1 σ) of the samples, calculated from the standards systematically interspersed in the analytical batches, were ±1.0 ‰ for $\delta^{15}N\text{-}NO_3^-$, ±1.5 ‰ for $\delta^{18}O\text{-}NO_3^-$, ±0.2 ‰ for $\delta^{15}N\text{-}N_{bulk}$, ±0.2 ‰ for $\delta^{13}C\text{-}C_{bulk}$, ±0.2 ‰ for $\delta^{13}C\text{-}DIC$, ±0.2 ‰ for $\delta^{34}S\text{-}SO_4^{2-}$, and ±0.5 ‰ for $\delta^{18}O\text{-}SO_4^{2-}$. Samples for chemical and isotopic analyses were prepared at the laboratory of the MAiMA-UB research group, and analyzed at the Centres Científics i Tecnològics of the Universitat de Barcelona (CCiT-UB).

3. RESULTS AND DISCUSSION

204 *3.1. Lab-scale evaluation of the nitrate removal capacities of compost, hay, and stubble at 24 ºC*

205 The chemical and isotopic characterization of the samples obtained from the laboratory
206 experiments are presented in the Supporting Information (**Table S3**). Although the intrinsic N
207 content measured in the three waste products (stubble, hay, and compost) were low (**Table 3**), it
208 was not possible to disregard a certain supply of N from these materials throughout the
209 incubations. The control microcosms containing the three C sources and DIW showed NO_3^-, NO_2^-
210 , and NH_4^+ concentrations below 0.09 mM, 0.02 mM, and 0.12 mM, respectively.

211 The biostimulation experiments showed that the three tested C sources were able to promote
212 NO_3^- removal. Complete denitrification (total NO_3^- and NO_2^- removal) was reached in
213 approximately 40 h in the microcosms containing stubble and hay, and in approximately 95 h in
214 that containing compost (**Figure 2A**). NH_4^+ was detected in some of the samples (in
215 concentrations of up to 1 mM), but with no clear pattern, suggesting the possible coexistence of
216 denitrification and dissimilatory NO_3^- reduction to NH_4^+ (DNRA) and/or the input of NH_4^+-N
217 supplied from the C sources tested. Transient NO_2^- accumulation of up to 1.5 mM (stubble and
218 hay) and 0.7 mM (compost) were observed. The highest concentration of NO_2^- in the stubble and
219 hay microcosms were detected after complete NO_3^- reduction, and subsequently decreased to
220 below the detectable limit in less than 40 h from the beginning of the experiment. Contrarily, in
221 the microcosms containing compost, the highest NO_2^- concentration was observed after 40 h,
222 and thereafter decreased along with NO_3^- concentration until both compounds were below the
223 detectable limits, after 96 h. The differences in NO_2^- accumulation between the compost, stubble,
224 and hay experiments were likely related to the rate of NO_3^- reduction. NO_2^- accumulation has
225 been reported to depend on the relative rates of NO_3^- and NO_2^- reduction (Betlach and Tiedje,
226 1981), as well as on the type of C source and C/N ratios employed (Akunna et al., 1993; Ge et
227 al., 2012). The slower reduction observed with compost could be due to the lower amount of
228 material used in the experiments (0.25 g instead of the 1 g used for stubble and hay). Although
229 the intrinsic C concentrations of the three sources were similar (**Table 3**), the C bioavailability
230 could differ between each product, and even between replicates, due to heterogeneity in the
231 materials (Breulmann et al., 2014; Sobczak and Findlay, 2002; Warneke et al., 2011).
232 Consequently, the NPDOC concentration did not show a clear correlation with NO_3^- reduction,
233 but provided an approximation of the amount of added C present in dissolved form. Although the

quantity of compost in the microcosms was only one-quarter of the quantity of vegetal materials used, the measured NPDOC concentrations in the three types of microcosms were similar (13.2-27.3 mM for stubble, 11.8-16.8 mM for hay, and 5.3-14.3 mM for compost). The δ^{13}C-DIC provided information about the transformation of organic C from the waste materials to inorganic C; a brief discussion is presented in the Supporting Information (**section S1**).

Concerning the safety of the materials, the ICP-OES analyses showed that there was no release of toxic trace elements from any of the tested compounds (Supporting Information **Table S4**). Hay and stubble seemed to be more feasible than compost for application in the CW. Compost resulted in a lower denitrification rate, the NO_2^- accumulation lasted longer, and it was highly soluble and could be rapidly removed from the CW via the water flow. In this study, stubble was selected for application in the studied CW due to a higher availability in the area. Therefore, further experiments were only performed with stubble.

3.2. Lab-scale evaluation of the effect of temperature on denitrification induction by stubble

The denitrification activity of microorganisms is usually increased with higher temperatures, and therefore higher NO_3^- attenuation from water can be observed during warm periods (Rivett et al., 2008; Spieles and Mitsch, 1999). To assess the effect of temperature on the induced denitrification strategy, additional experiments were performed. A comparison between different incubation temperatures in corn stubble experiments showed that denitrification reached completion across the whole temperature range studied (from 8 to 24 ºC), but with different lag periods and NO_3^- reduction rates. Complete denitrification was achieved after 40 h at 24 ºC, 65 h at 16 ºC, and 140 h at 8 ºC (**Figure 2B**). The decrease in NO_3^- began after 10 h at 24 ºC, whereas at 16 ºC and 8 ºC lag periods of 45 h and 79 h, respectively, were observed. A decrease in NO_3^- reduction rate associated with lower temperatures following the Arrhenius relationship has been well documented (Dawson and Murphy, 1972). Therefore, the denitrification efficiency might decrease during the winter months or low-temperature periods in comparison to that during the summer months, and thus application of the carbon source throughout the spring months might be advantageous. Significant transient NO_2^- accumulation (up to 1.5 mM at 24 ºC, 1.8 mM at 16 ºC, and 1.0 mM at 8 ºC) was observed in all the experiments. As discussed in the previous section, NO_2^- accumulation was less significant in the experiment with a lower denitrification rate (8 ºC).

3.3. Lab-scale assessment of the lifespan of the denitrification induced by stubble

One of the main issues associated with biostimulation strategies is their effectiveness during long-term treatments. It is thus important to consider the lifespan of the material to be employed in the CW. In another laboratory experiment with vegetable materials (palm leaves and compost), induced NO_3^- degradation was shown to be maintained for more than 220 d (Grau-Martínez et al., 2017). In this context, microcosms containing partially decomposed stubble (sampled in the CW 7.5 months after its application) were incubated and compared to microcosms containing fresh stubble. The denitrification induced by the partially decomposed stubble proceeded at a higher rate than that induced by the fresh stubble; complete NO_3^- reduction was achieved in less than 25 h with the former, instead of 40 h with the latter (**Figure 2B**). In the partially decomposed stubble microcosms, transient NO_2^- accumulation was below 0.8 mM. Due to the increased heterogeneity of the material after being in the field and in contact with water for months, high variabilities in both NO_3^- and NO_2^- concentrations were observed between replicates. Therefore, the reduction rates obtained from these experiments must be considered approximations. These results showed that the intrinsic capacity of the stubble to promote denitrification after 7.5 months being in contact with water was still important, at least at lab-scale. However, the NPDOC content in the microcosms containing partially decomposed stubble (1.7-8.8 mM) were lower than those in the microcosms with fresh stubble incubated at 24 ºC (13.2-27.3 mM), pointing to a decreased availability of the electron donor over time. In the CW, the specific lifespan of the treatment might be shorter, since the organic C also typically consumes O_2 before using NO_3^- as an electron donor. The N_2O accumulated in the headspace of the microcosms containing partially decomposed stubble incubated at 24 ºC (as well as that in the microcosms containing fresh stubble incubated at 16 and 8 ºC) was also measured since the release of greenhouse gases during N transformation processes is a matter of concern. The maximum N_2O concentration detected accounted for 0.015 % of the initial N-NO_3^- content of the microcosms (Supporting Information (**Table S3**)).

3.4. Lab-scale: NO_3^- isotopic fractionation calculation.

Under closed-system conditions, the isotopic fractionation (ε) for a determined element (e.g., N and O from dissolved NO_3^-) can be calculated by means of a Rayleigh distillation equation

(**Equation 1**). Thus, ε can be obtained from the slope of the linear correlation between the natural logarithm of the remaining substrate fraction ($Ln(C_{residual}/C_{initial})$, where C refers to analyte concentration) and the determined isotope ratios ($Ln(R_{residual}/R_{initial})$, where $R = \delta+1$). These $\varepsilon^{15}N_{NO3/N2}$ and $\varepsilon^{18}O_{NO3/N2}$ values, determined at lab-scale under controlled conditions, can be later applied at field-scale to estimate the contribution of denitrification to the NO_3^- attenuation, while avoiding field-scale interference such as dilution due to rainfall (Böttcher et al., 1990; Mariotti et al., 1988). We calculated $\varepsilon^{15}N_{NO3/N2}$ and $\varepsilon^{18}O_{NO3/N2}$ under all tested conditions at lab-scale (**Figure 3**) to appropriately evaluate the efficacy of the induced denitrification strategy tested at the CW. A summary of the calculated $\varepsilon^{15}N_{NO3/N2}$, $\varepsilon^{18}O_{NO3/N2}$, and $\varepsilon^{15}N/\varepsilon^{18}O$ values is shown in (**Table 4**); $\varepsilon^{15}N_{NO3/N2}$ ranged from -31.9 to -10.5‰, $\varepsilon^{18}O_{NO3/N2}$ from -30.4 to -9.7‰, and $\varepsilon^{15}N/\varepsilon^{18}O$ from 0.8 to 1.8. These values fall within the reported range for heterotrophic denitrification (see Table 4;Grau-Martínez et al., (2017)). The lowest $\varepsilon^{15}N_{NO3/N2}$ and $\varepsilon^{18}O_{NO3/N2}$ values were found for the microcosms containing compost incubated at 24 ºC and stubble incubated at 8 ºC, which were the two experiments that presented lower NO_3^- reduction rates. Apart from the microcosms containing stubble incubated at 8 ºC, the other microcosms containing stubble (both fresh and partially decomposed and incubated at 16 or 24 ºC) presented narrower ranges of $\varepsilon^{15}N_{NO3/N2}$ (from -28.3 to -22.5‰), $\varepsilon^{18}O_{NO3/N2}$ (from -30.4 to -21.2‰) and $\varepsilon^{15}N/\varepsilon^{18}O$ (from 0.8 to 1.1). These values were employed to assess the efficiency of the biostimulation strategy at the studied CW.

$$Ln\left(\frac{R_{residual}}{R_{initial}}\right) = \varepsilon \times Ln\left(\frac{C_{residual}}{C_{initial}}\right) \qquad \textbf{Equation 1}$$

3.5. Performance of the CW before application of stubble

The chemical and isotopic characterization of the samples obtained from the CW both before and after application of the electron donor are presented in Supporting Information (**Table S5**). Three sampling campaigns were performed at the CW before stubble application. While NO_3^- was not significantly reduced during the two sampling campaigns performed at a ~5.5 L/s flow rate (June and September 2017), a slight attenuation (from 1.3 to 0.8 mM) occurred under operation at ~2.5 L/s (September 2017) (**Figure 4A**). In all samples, NO_2^- was below the detection limit and NH_4^+ was below 0.01 mM, suggesting that NO_3^- had been either transformed to gaseous N products through denitrification or assimilated by plants or microorganisms (Supporting information (**Table S5)**). Whereas no increase in $\delta^{15}N\text{-}NO_3^-$ nor $\delta^{18}O\text{-}NO_3^-$ was observed in the samples collected

during the first campaign at ~5.5 L/s (June 14, 2017), an increase was observed at the middle section of the CW (H3) during the second survey at ~5.5 L/s (September 5, 2017). In this latter campaign, the inlet (H1) presented $\delta^{15}N\text{-}NO_3^-$ and $\delta^{18}O\text{-}NO_3^-$ values of +11.6 ‰ and +8.7 ‰, respectively, which increased at the middle point (H3) up to +19.2 ‰ and +18.2 ‰, respectively, and decreased at the outlet (H6) to +9.6 ‰ and +7.1 ‰, respectively (**Figure 4B**). A proposed explanation is that the occurrence of preferential flows within the wetland (e.g., heterogeneous flow rate between surface and bottom water or between lateral and central water) could have led to an increased hydraulic retention time and/or stagnant water at the H3 sampling site. In the campaign performed at a ~2.5 L/s flow rate (September 12, 2017), the decrease in NO_3^- concentration was coupled to increases in $\delta^{15}N\text{-}NO_3^-$ and $\delta^{18}O\text{-}NO_3^-$ from the inlet (+7.0 ‰ and +4.7 ‰, respectively, at H1) to the outlet (+17.1 ‰ and +13.0 ‰, respectively, at H6) of the CW (**Figure 4B**). The slope of the relation between $\delta^{18}O\text{-}NO_3^-$ and $\delta^{15}N\text{-}NO_3^-$ for the samples collected in these three campaigns was 0.8 (r^2 = 0.91) (**Figure 4B**), which is indicative of denitrification activity (Aravena et al., 1998). These results are in agreement with previous results reporting the occurrence of denitrification in CWs even in the presence of dissolved O_2 (Sirivedhin and Gray, 2006). The intrinsic denitrification activity in the CW did not support complete denitrification, likely due to the low NPDOC content of the water (0.4 – 0.6 mM). Therefore, it was decided to evaluate the feasibility of adding an external electron donor source to promote NO_3^- attenuation when operating at a ~16 L/s flow rate.

3.6. Performance of the CW after application of stubble

Application of stubble in autumn (September 25, 2017) induced denitrification in the CW approximately 2 d after the application (**Figure 5B**). Denitrification was almost complete at the outlet (H6) by 14 d following the application (0.2 mM NO_3^- remaining of the initial 1.4 – 1.7 mM) (**Figure 5A**). In the two sampling campaigns, NO_2^- accumulated beginning at H2 and reached a concentration of 0.2 mM by the outlet (H6) by 7 d after treatment, but decreased to 0.1 mM by 14 d. Such a decrease in NO_2^- accumulation over time has been previously observed in laboratory experiments and other denitrification studies (Carrey et al., 2014; Margalef-Marti et al., 2019; Vidal-Gavilan et al., 2013). The maximum NH_4^+ concentration of 0.02 mM was measured at H3 after 7 d, while it decreased by the outlet (H6) to 0.01 mM in both campaigns, pointing to a non-significant contribution of DNRA. Due to the application of stubble, the outlet flow rate decreased

until the system became partially blocked, leaving the monitoring probes exposed to the air. When the problem was solved (October 17, 2017) and the outlet flow was stabilized at approximately 16 L/s, the NO_3^- concentration monitored at the outlet showed fluctuations, pointing to a slight denitrification activity until October 24, 2017 (**Figure 5C**). Thus, the lifetime of the treatment in autumn (recorded temperatures in October 2017 ranged from 10.3 ºC to 20.4 ºC, averaging 16.0 ºC) was estimated to be between 2 weeks and 1 month.

Application of stubble in spring (May 5, 2018) also induced denitrification and underwent a shorter acclimation time (1 d) with respect to the first application, likely due to faster acclimation by the previously stimulated bacterial community (**Figure 6A**). By 7 d after the stubble application, the NO_3^- concentration at the outlet (H6) was 0.2 mM, and denitrification was complete after 14 d. The NO_3^- concentration in the outlet then began to increase progressively until reaching a level similar to that at the inlet by approximately 100 d after treatment (**Figure 6B**). A lower NO_3^- concentration measured in H3 during the last sampling campaign (+161 d) was attributed to stagnant water near the sampling point due to the accumulation of partially decomposed stubble. Thus, the treatment in spring-summer (temperatures recorded from May to October 2018 presented monthly minimums from 9.6 to 19.9 ºC, monthly maximums from 20.0 to 28.4 ºC, and monthly averages from 15.8 to 24.6 ºC) induced significant denitrification for approximately three months, which is three times longer than that induced by the treatment in autumn. The NO_3^- concentration decrease at the outlet compared to inlet during these three months ranged from 0.1 to 1.5 mM (highest attenuation corresponded to the first month after stubble application). All the monitored NO_3^- concentrations at the inlet and outlet of the CW during this study period are presented in the Supporting Information **Figure S1**. The increased efficiency of the treatment in spring-summer compared to that of the treatment in autumn is in accordance with laboratory results (incubation at 8, 16, and 24 ºC) and with previous wetland studies reporting increased denitrification rates at higher temperatures (Bachand and Horne, 1999; Christensen and Srensen, 1986; Si et al., 2018). The faster acclimation by the previously stimulated bacterial community could have been also responsible for this increased attenuation activity.

After the second stubble application, 0.1 mM of NO_2^- was detected at the outlet (H6) for 63 d. Afterwards, it was no longer detected (except at the aforementioned point H3 where water stagnated), confirming a decreased NO_2^- accumulation with time as observed during the previous

381 treatment period. The maximum NH_4^+ concentration detected, 0.3 mM, was recorded at H4 7 d
382 after application, while at the outlet (H6), the concentration was 0.05 mM. At 14 d and one month
383 after application, NH_4^+ at the outlet decreased to 0.02 mM and 0.01 mM, respectively. These
384 results suggest that transient DNRA activity could have arisen between H2 and H4 following the
385 stubble application. NO_3^- is reduced to NH_4^+ through DNRA, depending on parameters such as
386 microbial growth rate, NO_2^- accumulation, and the C:N ratio (Kraft et al., 2014). It is generally
387 accepted that DNRA is favored at high C:N ratios, when NO_3^- is limited (rather than the electron
388 donor being limited), or when high NO_3^- levels inhibit NO_2^- reductase (Giles et al., 2012; Kelso et
389 al., 1997). This hypothesis is consistent with the higher degree of NH_4^+ accumulation observed
390 in laboratory experiments compared to that observed in the field, since higher C:N ratios with a
391 more homogeneous distribution were found in the batch experiments. It is also necessary to
392 account for the possible input of N from the applied stubble. NO_2^- and NH_4^+ have a lower threshold
393 for human consumption (0.01 and 0.03 mM, respectively) with respect to that of NO_3^- (0.8 mM)
394 (98/83/EC, 1998). However, since NH_4^+ accumulation decreased before the outlet and fell to
395 insignificant levels by 14 d after treatment, and the NO_2^- accumulation also decreased over time,
396 stubble was considered effective in removing N compounds from agricultural runoff water.

397 A few authors have previously attempted to calculate the denitrification efficiency in CWs by
398 means of isotopic assessment, but using ε values available in the literature and only for $N\text{-}NO_3^-$
399 (Lund et al., 1999; Søvik and Mørkved, 2008). The $\varepsilon^{15}N_{NO3/N2}$ and $\varepsilon^{18}O_{NO3/N2}$ values obtained from
400 our lab-scale experiments in which fresh stubble was incubated at 24 and 16 ºC, and partially
401 decomposed stubble was incubated at 24 ºC, were used to calculate three denitrification % lines
402 (**Equation 2**, derived from **Equation 1**) that were plotted on a graph of $\delta^{18}O\text{-}NO_3^-$ versus $\delta^{15}N\text{-}$
403 NO_3^- along with the isotopic results for the CW samples (**Figure 7**). These three laboratory
404 conditions encompass the average temperatures recorded during the biostimulation periods
405 tested at the CW. The slope of $\delta^{18}O\text{-}NO_3^-$ versus $\delta^{15}N\text{-}NO_3^-$ for the field samples collected after
406 the biostimulation treatment was 1.0 (r^2 = 0.98) (**Figure 7**), which is slightly higher than that
407 obtained for the intrinsic denitrification before the stubble addition (0.8 (r^2 = 0.91)), which is likely
408 due to the use of a different C source and the promotion of a different bacterial community. Also,
409 the slope obtained after the biostimulation (1.0) was similar to the slopes obtained in the lab-scale
410 experiments using partially decomposed stubble incubated at 24 ºC (0.9) and those using fresh

stubble incubated at 24 and 16 ºC (1.25 and 1.1, respectively). This is consistent with the temperatures registered in the area throughout the test period, and with the stubble being in contact with water. This similarity between the field-scale and lab-scale slopes, together with the observed isotopic fractionation in the CW suggested that plant uptake did not likely contribute significantly to the NO_3^- removal.

$$\text{Denitrification \%} = \left[1 - \left(\frac{C_{residual}}{C_{initial}}\right)\right] \times 100 = \left[1 - e^{\left(\frac{\delta_{residual} - \delta_{initial}}{\varepsilon}\right)}\right] \times 100$$

Equation 2

The results showed that at least 60% of NO_3^- attenuation was achieved in the CW due to the induced denitrification, although this value was obtained from the less-favorable situation (where the denitrification % was calculated from the experiments using stubble incubated at 24 ºC). If the denitrification % is instead calculated based on the experiment using partially decomposed stubble incubated at 24 ºC, which presents the slope most similar to that of the field samples (0.9 compared to 1.0), then denitrification accounted for a 70 % NO_3^- removal. The largest contribution of denitrification, as determined by isotopic data, was observed in the outlet samples (H6) taken 7 and 14 d after the first stubble application, and 7 d after the second stubble application. By 14 d after the second stubble application, NO_3^- concentration in some samples was below the level required for the isotopic analysis. Therefore, the induced denitrification allowed a NO_3^- attenuation close to 100 %. After two weeks of treatment, the contribution of the induced denitrification at the outlet (H6) began to decrease, from 30 % in June 2018 to 5 % in September 2018, and slightly increased to 20 % by the last survey in October 2018. Considering an average flow rate of 16 L/s (the application of stubble led to fluctuations in the flow rate due to partial blockages at some points caused by stubble accumulation) and these results, in the studied CW, at least 80 kg of NO_3^- were removed per day over the first two weeks after the stubble application in May 2018 and 30 kg/d were removed from 14 to 63 d after the supply, after which time the removal decreased. A comparison between the denitrification percentages calculated using chemical and isotopic data revealed that using concentration values always resulted in a higher value. Since the contribution calculated from the isotopic data was considered to be linked to NO_3^- attenuation due to denitrification, the difference could be due to a decrease in NO_3^- concentration provoked by dilution due to precipitation, or the contribution of plant uptake to NO_3^- attenuation.

3.7. Effect and evolution of NPDOC in the CW

Since the amount of organic C released from the CW to the Lerma gully, and from there to the Arba River was a matter of concern, the NPDOC concentration in the field samples were measured. Only the results obtained from the second stubble application are discussed (the first application gave similar results). The NPDOC concentration at the outlet increased with respect to the background values by 7 d after application, and the increased level was maintained for 14 d in total (**Figure 8**). The increase began at H3, reached a maximum between H4 and H5 (1.6 – 1.7 mM), and decreased to approximately 1.0 – 1.1 mM by the outlet (H6), indicating a release of organic C to the gully (background NPDOC concentrations ranged from 0.5 to 0.8 mM). Because the gully contained NO_3^--polluted water, it was considered that the surplus organic C could lead to NO_3^- attenuation downstream. The high NPDOC concentration detected between H3 and H5 could have provoked a decrease in water quality within the CW due to the promotion of processes such as DNRA (previously discussed) and bacterial SO_4^{2-} reduction (BSR), through which NH_4^+ and H_2S are produced, respectively. Although BSR is usually induced when NO_3^- is completely removed from the environment, the coexistence of denitrification and BSR in the presence of an abundance of an electron donor has also been demonstrated (Laverman et al., 2012). The isotopic characterization of SO_4^{2-} can provide information to assess its transformation processes because the decrease in SO_4^{2-} concentration is coupled to increases in δ^{34}S-SO_4^{2-} and δ^{18}O-SO_4^{2-} through the BSR (Strebel et al., 1990). Correlation between SO_4^{2-} concentration and isotopic composition was not identified in the samples collected at the CW, suggesting that BSR was not occurring in the CW. Therefore, the possibility of a decrease in water quality in the CW due to H_2S production as a result of excess organic C was discarded.

3.8. Suitability of the strategy and future improvements

The remediation strategy tested in the CW allowed the induction of the removal of NO_3^- from agricultural runoff water. The NO_3^- attenuation was primarily related to denitrification. Previous studies also found that denitrification was an important N sink in CWs in comparison to plant uptake (Lin et al., 2002; Soana et al., 2017). It has to be considered that denitrification can only be considered a N sink if intermediate products such as NO_2^- or N_2O are not accumulated during the NO_3^- reduction. The added stubble could have enhanced denitrification not only by increasing

469 the organic C content of the water but also by inhibiting O_2 production through photosynthesis by
470 shading the water column, as previously hypothesized by Jacobs and Harrison (2014) for floating
471 vegetation in CWs. However, the denitrification efficiency was limited. The most likely explanation
472 involves the high O_2 content of the inlet water (near saturation, approximately 0.28 and 0.34 mM
473 in summer and winter, respectively) (Merchán et al., 2014) and the vast surface available for O_2
474 diffusion. Other parameters that could have also contributed to the limited denitrification efficiency
475 include the high water flow rate tested in the CW (~16 L/s), and the possible generation of
476 preferential flows within the CW (e.g., due to stubble accumulation in some points) that could led
477 to a low degree of interaction between water and stubble.

478 Although application of solid residues such as maize stubble in surface flow CWs might have
479 advantages over the application of liquid organic C sources, which face the problems of greater
480 loss by bacterial oxidation (Lin, 2002) and greater release with the water flow, new strategies for
481 increasing the lifespan and efficacy of the induced denitrification must be investigated. In addition,
482 increased intrinsic denitrification capacity of the CW is expected after plant growth covers the
483 entire surface. Previous studies have reported increased denitrification activity in vegetated CWs
484 relative to the levels in non-vegetated systems (Lin et al., 2002; Soana et al., 2017), with efficacy
485 varying among plants of different species or age (Lin et al., 2002; Lund et al., 1999). The organic
486 C pool released after plant senescence has also been demonstrated to increase the bacterial
487 activity, as this C can also be used as electron donor (Peralta et al., 2012; Soana et al., 2017). In
488 this direction, Kang et al. (2018) proposed the use of plants whose growth season is winter.
489 Therefore, the organic C supply from senescence would occur throughout the summer months,
490 when temperatures are higher and more appropriate conditions are established for the promotion
491 of significant denitrification activity.

492 N_2O production was not assessed in our field-scale tests. At lab-scale, limited N_2O production
493 was observed. However, at field-scale, higher N_2O emissions could occur as a result of
494 denitrification induced by the stubble addition because the high O_2 content of the inlet water and
495 the free surface water flow might allow more extensive O_2 diffusion in water. Since N_2O emissions
496 are detrimental for air quality, the production of this greenhouse gas should also be monitored in
497 treatments aiming to induce denitrification. Isotopic characterization of the N_2O emitted from a

given CW could also provide further information about the N transformation processes that led to the decrease in NO_3^- concentration.

4. CONCLUSIONS

At laboratory-scale, maize stubble, wheat hay, and animal compost were able to induce complete denitrification. Stubble was selected for field-scale application due to its better local availability. In the following incubations, stubble sampled from the CW 7.5 months after its application was still able to support complete NO_3^- attenuation. Complete NO_3^- attenuation was achieved over the temperature range of 8 to 24 ºC, although lower temperatures resulted in lower reduction rates. The $\varepsilon^{15}N_{NO3/N2}$ and $\varepsilon^{18}O_{NO3/N2}$ values obtained from the laboratory experiments allowed evaluation of the performance of the remediation strategy at the CW.

Before the application of the stubble, NO_3^- attenuation at the CW (from 1.3 to 0.8 mM) was only observed when the flow was decreased from approximately 5.5 to 2.5 L/s. The biostimulation in autumn-winter promoted NO_3^- attenuation lasting between 2 weeks and one month, while in spring-summer the attenuation capacity remained for approximately three months (~16 L/s flow rate). The isotopic characterization of the CW samples indicated that at least 60 % of the initial NO_3^- was removed in the CW due to the induced denitrification. However, since in a few samples NO_3^- was below the limit necessary for isotopic analysis, the contribution could have been higher. The slope of $\delta^{18}O\text{-}NO_3^-$ versus $\delta^{15}N\text{-}NO_3^-$ obtained in the CW after the stubble application (1.0) was close to that obtained in the experiments involving partially decomposed stubble incubated at 24ºC (1.1). Plant uptake seemed to play only a minor role in NO_3^- attenuation in the CW. The treatment was considered safe because NO_2^- and NH_4^+ accumulation (below 0.2 and 0.1 mM, respectively) decreased over time, surplus NPDOC (below 2.3 mM) released from the CW could maintain NO_3^- attenuation downstream, and because the occurrence of BSR was discarded. However, the longevity and effectivity of the treatment were limited due to the high O_2 content of the inlet water, high water flow, and the possible generation of preferential flows within the CW.

ACKNOWLEDGEMENTS

This work was financed by the projects REMEDIATION (CGL2014-57215-C4), AGRO-SOS (CGL2015-66016-R) and PACE-ISOTEC (CGL2017-87216-C4-1-R) financed by the Spanish

Government and AEI/FEDER financed by the European Union, and by MAG (2017 SGR 1733) financed by the Catalan Government. R. Margalef-Marti thanks the Spanish Government for the Ph.D. grant BES-2015-072882. D. Merchán was supported by the "Juan de la Cierva – Formación" program (FJCI-2018-24920). We would also like to thank the CCiT of the Universitat the Barcelona for the analytical support, and A. Fernández for his contribution to the study.

REFERENCES

91/676/EEC, 1991. Nitrates Directive. Council Directive 91/676/EEC of 12 December 1991, concerning the protection of waters against pollution caused by nitrates from agricultural sources. [WWW Document]. Off. J. Eur. Comm. URL http://ec.europa.eu/environment/index_en.htm (accessed 4.9.17).

98/83/EC, 1998. Drinking Water Directive. Council Directive 98/83/EC, of 3 November 1998, on the quality of water intended for human consumption. [WWW Document]. Off. J. Eur. Comm. URL http://ec.europa.eu/environment/index_en.htm (accessed 4.9.17).

Akunna, J.C., Bizeau, C., Moletta, R., 1993. Nitrate and nitrite reductions with anaerobic sludge using various carbon sources: Glucose, glycerol, acetic acid, lactic acid and methanol. Water Res. 27, 1303–1312. https://doi.org/10.1016/0043-1354(93)90217-6

Aravena, R., Robertson, W.D., 1998. Use of multiple isotope tracers to evaluate denitrification in ground water: study of nitrate from a large-flux septic system plume. Ground Water 36, 975–982.

Bachand, P.A.M., Horne, A.J., 1999. Denitrification in constructed free-water surface wetlands: I. Very high nitrate removal rates in a macrocosm study. Ecol. Eng. 14, 9–15. https://doi.org/10.1016/S0925-8574(99)00016-6

Betlach, M.R., Tiedje, J.M., 1981. Kinetic Explanation for Accumulation of Nitrite, Nitric Oxide, and Nitrous Oxide during Bacterial Denitrification. Appl. Environ. Microbiol. 42, 1074–1084. https://doi.org/Article

Beutel, M.W., Newton, C.D., Brouillard, E.S., Watts, R.J., 2009. Nitrate removal in surface-flow constructed wetlands treating dilute agricultural runoff in the lower Yakima Basin,

553 Washington. Ecol. Eng. 35, 1538–1546. https://doi.org/10.1016/j.ecoleng.2009.07.005

554 Böttcher, J., Strebel, O., Voerkelius, S., Schmidt, H.L., 1990. Using isotope fractionation of
555 nitrate-nitrogen and nitrate-oxygen for evaluation of microbial denitrification in a sandy
556 aquifer. J. Hydrol. 114, 413–424. https://doi.org/10.1016/0022-1694(90)90068-9

557 Breulmann, M., Masyutenko, N.P., Kogut, B.M., Schroll, R., Dörfler, U., Buscot, F., Schulz, E.,
558 2014. Short-term bioavailability of carbon in soil organic matter fractions of different
559 particle sizes and densities in grassland ecosystems. Sci. Total Environ. 497–498, 29–37.
560 https://doi.org/10.1016/j.scitotenv.2014.07.080

561 Carrey, R., Otero, N., Vidal-Gavilan, G., Ayora, C., Soler, A., Gómez-Alday, J.J., 2014. Induced
562 nitrate attenuation by glucose in groundwater: Flow-through experiment. Chem. Geol. 370,
563 19–28. https://doi.org/10.1016/j.chemgeo.2014.01.016

564 Carrey, R., Rodríguez-Escales, P., Soler, A., Otero, N., 2018. Tracing the role of endogenous
565 carbon in denitrification using wine industry by-product as an external electron donor:
566 Coupling isotopic tools with mathematical modeling. J. Environ. Manage. 207, 105–115.
567 https://doi.org/10.1016/j.jenvman.2017.10.063

568 Christensen, P.B., Srensen, J.A.N., 1986. Temporal Variation of Denitrification Activity in Plant-
569 Covered , Littoral Sediment from Lake Hampen , Denmark 51, 1174–1179.

570 Cooper, A.B., Cooke, J.G., 1984. Nitrate loss and transformation in 2 vegetated headwater
571 streams. New Zeal. J. Mar. Freshw. Res. 18, 441–450.
572 https://doi.org/10.1080/00288330.1984.9516065

573 Coplen, T.B., 2011. Guidelines and recommended terms for expression of stable-isotope-ratio
574 and gas-ratio measurement results. Rapid Commun. Mass Spectrom. 25, 2538–2560.
575 https://doi.org/10.1002/rcm.5129

576 Dawson, R.N., Murphy, K.L., 1972. The temperature dependency of biological denitrification.
577 Water Res. 6, 71–83. https://doi.org/10.1016/0043-1354(72)90174-1

578 Dogramaci, S.., Herczeg, A.., Schiff, S.., Bone, Y., 2001. Controls on $\delta^{34}S$ and $\delta^{18}O$ of dissolved
579 sulfate in aquifers of the Murray Basin, Australia and their use as indicators of flow

processes. Appl. Geochemistry 16, 475–488. https://doi.org/10.1016/S0883-2927(00)00052-4

Estrada, N.L., Böhlke, J.K., Sturchio, N.C., Gu, B., Harvey, G., Burkey, K.O., Grantz, D.A., McGrath, M.T., Anderson, T.A., Rao, B., Sevanthi, R., Hatzinger, P.B., Jackson, W.A., 2017. Stable isotopic composition of perchlorate and nitrate accumulated in plants: Hydroponic experiments and field data. Sci. Total Environ. 595, 556–566. https://doi.org/10.1016/j.scitotenv.2017.03.223

Fukada, T., Hiscock, K.M., Dennis, P.F., Grischek, T., 2003. A dual isotope approach to identify denitrification in groundwater at a river-bank infiltration site. Water Res. 37, 3070–3078. https://doi.org/10.1016/S0043-1354(03)00176-3

Ge, S., Peng, Y., Wang, S., Lu, C., Cao, X., Zhu, Y., 2012. Nitrite accumulation under constant temperature in anoxic denitrification process: The effects of carbon sources and COD/NO3-N. Bioresour. Technol. 114, 137–143. https://doi.org/10.1016/j.biortech.2012.03.016

Giles, M., Morley, N., Baggs, E.M., Daniell, T.J., 2012. Soil nitrate reducing processes - Drivers, mechanisms for spatial variation, and significance for nitrous oxide production. Front. Microbiol. 3, 1–16. https://doi.org/10.3389/fmicb.2012.00407

Grau-Martínez, A., Torrentó, C., Carrey, R., Rodríguez-Escales, P., Domènech, C., Ghiglieri, G., Soler, A., Otero, N., 2017. Feasibility of two low-cost organic substrates for inducing denitrification in artificial recharge ponds: Batch and flow-through experiments. J. Contam. Hydrol. 198, 48–58. https://doi.org/10.1016/j.jconhyd.2017.01.001

Gumbricht, T., 1993. Nutrient removal capacity in submersed macrophyte pond systems in a temperature climate. Ecol. Eng. 2, 49–61. https://doi.org/10.1016/0925-8574(93)90026-C

Ilyas, H., Masih, I., 2017. The performance of the intensified constructed wetlands for organic matter and nitrogen removal: A review. J. Environ. Manage. 198, 372–383. https://doi.org/10.1016/j.jenvman.2017.04.098

Jacobs, A.E., Harrison, J.A., 2014. Effects of floating vegetation on denitrification, nitrogen

retention, and greenhouse gas production in wetland microcosms. Biogeochemistry 119, 51–66. https://doi.org/10.1007/s10533-013-9947-9

Kang, Y., Zhang, J., Li, B., Zhang, Y., Sun, H., Hao Ngo, H., Guo, W., Xie, H., Hu, Z., Zhao, C., 2018. Improvement of bioavailable carbon source and microbial structure toward enhanced nitrate removal by Tubifex tubifex. Chem. Eng. J. 353, 699–707. https://doi.org/10.1016/j.cej.2018.07.182

Kelso, B.H.L., Smith, R. V., Laughlin, R.J., Lennox, S.D., 1997. Dissimilatory nitrate reduction in anaerobic sediments leading to river nitrite accumulation. Appl. Environ. Microbiol. 63, 4679–4685.

Knowles, R., 1982. Denitrification. Microbiol. Rev. 46, 43–70.

Kong, L., Wang, Y. Bin, Zhao, L.N., Chen, Z.H., 2009. Enzyme and root activities in surface-flow constructed wetlands. Chemosphere 76, 601–608. https://doi.org/10.1016/j.chemosphere.2009.04.056

Kovacic, D.A., David, M.B., Gentry, L.E., Starks, K.M., Cooke, R.A., 2000. Effectiveness of Constructed Wetlands in Reducing Nitrogen and Phosphorus Export from Agricultural Tile Drainage. J. Environ. Qual. 29, 1262. https://doi.org/10.2134/jeq2000.00472425002900040033x

Kraft, B., Tegetmeyer, H.E., Sharma, R., Klotz, M.G., Ferdelman, T.G., Hettich, R.L., Geelhoed, J.S., Strous, M., 2014. The environmental controls that govern the end product of bacterial nitrate respiration. Science (80). 345, 3–7.

Laverman, A.M., Pallud, C., Abell, J., Cappellen, P. Van, 2012. Comparative survey of potential nitrate and sulfate reduction rates in aquatic sediments. Geochim. Cosmochim. Acta 77, 474–488. https://doi.org/10.1016/j.gca.2011.10.033

Lin, Y.F., Jing, S.R., Wang, T.W., Lee, D.Y., 2002. Effects of macrophytes and external carbon sources on nitrate removal from groundwater in constructed wetlands. Environ. Pollut. 119, 413–420. https://doi.org/10.1016/S0269-7491(01)00299-8

Lu, S., Hu, H., Sun, Y., Yang, J., 2009. Effect of carbon source on the denitrification in

constructed wetlands. J. Environ. Sci. 21, 1036–1043. https://doi.org/10.1016/S1001-0742(08)62379-7

Lund, L.., Horne, A.., Williams, A.., 1999. Estimating denitrification in a large constructed wetland using stable nitrogen isotope ratios. Ecol. Eng. 14, 67–76. https://doi.org/10.1016/S0925-8574(99)00020-8

Margalef-Marti, R., Carrey, R., Soler, A., Otero, N., 2019. Evaluating the potential use of a dairy industry residue to induce denitrification in polluted water bodies: A flow-through experiment. J. Environ. Manage. 245. https://doi.org/10.1016/j.jenvman.2019.03.086

Mariotti, A., Germon, J.C., Hubert, P., Kaiser, P., Letolle, R., Tardieux, A., Tardieux, P., 1981. Experimental determination of nitrogen kinetic isotope fractionation: Some principles; illustration for the denitrification and nitrification processes. Plant Soil 62, 413–430. https://doi.org/10.1007/BF02374138

Mariotti, A., Landreau, A., Simon, B., 1988. ^{15}N isotope biogeochemistry and natural denitrification process in groundwater: Application to the chalk aquifer of northern France. Geochim. Cosmochim. Acta 52, 1869–1878. https://doi.org/10.1016/0016-7037(88)90010-5

McIlvin, M.R., Altabet, M.A., 2005. Chemical conversion of nitrate and nitrite to nitrous oxide for nitrogen and oxygen isotopic analysis in freshwater and seawater. Anal Chem 77, 5589–5595. https://doi.org/10.1021/ac050528s

Merchán, D., Causapé, J., Abrahão, R., 2013. Impact of irrigation implementation on hydrology and water quality in a small agricultural basin in Spain. Hydrol. Sci. J. 58, 1400–1413. https://doi.org/10.1080/02626667.2013.829576

Merchán, D., Causapé, J., Abrahão, R., García-Garizábal, I., 2015. Assessment of a newly implemented irrigated area (Lerma Basin, Spain) over a 10-year period. II: Salts and nitrate exported. Agric. Water Manag. https://doi.org/10.1016/j.agwat.2015.04.019

Merchán, D., Otero, N., Soler, A., Causapé, J., 2014. Main sources and processes affecting dissolved sulphates and nitrates in a small irrigated basin (Lerma Basin, Zaragoza, Spain):

Isotopic characterization. Agric. Ecosyst. Environ. 195, 127–138. https://doi.org/10.1016/j.agee.2014.05.011

Peralta, A.L., Matthews, J.W., Flanagan, D.N., Kent, A.D., 2012. Environmental factors at dissimilar spatial scales influence plant and microbial communities in restored wetlands. Wetlands 32, 1125–1134. https://doi.org/10.1007/s13157-012-0343-3

Rivett, M.O., Buss, S.R., Morgan, P., Smith, J.W.N., Bemment, C.D., 2008. Nitrate attenuation in groundwater: A review of biogeochemical controlling processes. Water Res. 42, 4215–4232. https://doi.org/10.1016/j.watres.2008.07.020

Rogers, K.H., Breen, P.F., Chick, A.J., 1991. Nitrogen Removal in Experimental Wetland Treatment Systems: Evidence for the Role of Aquatic Plants. Res. J. Water Pollut. Control Fed. 63, 934–941.

Ryabenko, E., Altabet, M. a., Wallace, D.W.R., 2009. Effect of chloride on the chemical conversion of nitrate to nitrous oxide for $\delta^{15}N$ analysis. Limnol. Oceanogr. Methods 7, 545–552. https://doi.org/10.4319/lom.2009.7.545

Scott, J.T., McCarthy, M.J., Gardner, W.S., Doyle, R.D., 2008. Denitrification, dissimilatory nitrate reduction to ammonium, and nitrogen fixation along a nitrate concentration gradient in a created freshwater wetland. Biogeochemistry 87, 99–111. https://doi.org/10.1007/s10533-007-9171-6

Si, Z., Song, X., Wang, Y., Cao, X., Zhao, Y., Wang, B., Chen, Y., Arefe, A., 2018. Intensified heterotrophic denitrification in constructed wetlands using four solid carbon sources: Denitrification efficiency and bacterial community structure. Bioresour. Technol. 267, 416–425. https://doi.org/10.1016/j.biortech.2018.07.029

Sirivedhin, T., Gray, K.A., 2006. Factors affecting denitrification rates in experimental wetlands: Field and laboratory studies. Ecol. Eng. 26, 167–181. https://doi.org/10.1016/j.ecoleng.2005.09.001

Soana, E., Balestrini, R., Vincenzi, F., Bartoli, M., Castaldelli, G., 2017. Mitigation of nitrogen pollution in vegetated ditches fed by nitrate-rich spring waters. Agric. Ecosyst. Environ.

688 243, 74–82. https://doi.org/10.1016/j.agee.2017.04.004

689 Sobczak, W. V., Findlay, S., 2002. Variation in Bioavailability of Dissolved Organic Carbon
690 among Stream Hyporheic Flowpaths. Ecology 83, 3194–3209.

691 Søvik, A.K., Mørkved, P.T., 2008. Use of stable nitrogen isotope fractionation to estimate
692 denitrification in small constructed wetlands treating agricultural runoff. Sci. Total Environ.
693 392, 157–165. https://doi.org/10.1016/j.scitotenv.2007.11.014

694 Spieles, D.J., Mitsch, W.J., 1999. The effects of season and hydrologic and chemical loading on
695 nitrate retention in constructed wetlands: A comparison of low- and high-nutrient riverine
696 systems. Ecol. Eng. 14, 77–91. https://doi.org/10.1016/S0925-8574(99)00021-X

697 Spoelstra, J., Schiff, S.L., Semkin, R.G., Jeffries, D.S., Elgood, R.J., 2010. Nitrate attenuation in
698 a small temperate wetland following forest harvest. For. Ecol. Manage. 259, 2333–2341.
699 https://doi.org/10.1016/j.foreco.2010.03.006

700 Strebel, O., Böttcher, J., Fritz, P., 1990. Use of isotope fractionation of sulfate-sulfur and sulfate-
701 oxygen to assess bacterial desulfurication in a sandy aquifer. J. Hydrol. 121, 155–172.
702 https://doi.org/10.1016/0022-1694(90)90230-U

703 Tanner, C.C., Nguyen, M.L., Sukias, J.P.S., 2005. Nutrient removal by a constructed wetland
704 treating subsurface drainage from grazed dairy pasture. Agric. Ecosyst. Environ. 105,
705 145–162. https://doi.org/10.1016/j.agee.2004.05.008

706 Trois, C., Coulon, F., de Combret, C.P., Martins, J.M.F., Oxarango, L., 2010. Effect of pine bark
707 and compost on the biological denitrification process of non-hazardous landfill leachate:
708 Focus on the microbiology. J. Hazard. Mater. 181, 1163–1169.
709 https://doi.org/10.1016/j.jhazmat.2010.05.077

710 Uusheimo, S., Tulonen, T., Aalto, S.L., Arvola, L., 2018. Mitigating agricultural nitrogen load with
711 constructed ponds in northern latitudes: A field study on sedimental denitrification rates.
712 Agric. Ecosyst. Environ. 261, 71–79. https://doi.org/10.1016/j.agee.2018.04.002

713 Vidal-Gavilan, G., Folch, A., Otero, N., Solanas, A.M., Soler, A., 2013. Isotope characterization
714 of an in situ biodenitrification pilot-test in a fractured aquifer. Appl. Geochemistry 32, 153–

163. https://doi.org/10.1016/j.apgeochem.2012.10.033

Vitousek, P.M., Aber, J.D., Howarth, R.W., Likens, G.E., Matson, P.A., Schindler, D.W., Schlesinger, W.H., Tilman, D.G., 1997. Summary for Policymakers, in: Intergovernmental Panel on Climate Change (Ed.), Climate Change 2013 - The Physical Science Basis. Cambridge University Press, Cambridge, pp. 1–30. https://doi.org/10.1017/CBO9781107415324.004

Vymazal, J., 2007. Removal of nutrients in various types of constructed wetlands. Sci. Total Environ. 380, 48–65. https://doi.org/10.1016/j.scitotenv.2006.09.014

Ward, M.H., DeKok, T.M., Levallois, P., Brender, J., Gulis, G., Nolan, B.T., VanDerslice, J., 2005. Workgroup Report: Drinking-Water Nitrate and Health—Recent Findings and Research Needs. Environ. Health Perspect. 113, 1607–1614. https://doi.org/10.1289/ehp.8043

Warneke, S., Schipper, L.A., Matiasek, M.G., Scow, K.M., Cameron, S., Bruesewitz, D.A., McDonald, I.R., 2011. Nitrate removal, communities of denitrifiers and adverse effects in different carbon substrates for use in denitrification beds. Water Res. 45, 5463–5475. https://doi.org/10.1016/j.watres.2011.08.007

Wu, H., Zhang, J., Ngo, H.H., Guo, W., Hu, Z., Liang, S., Fan, J., Liu, H., 2015. A review on the sustainability of constructed wetlands for wastewater treatment: Design and operation. Bioresour. Technol. 175, 594–601. https://doi.org/10.1016/j.biortech.2014.10.068

Figure 1. CW design. Photograph of the surface flow CW with emergent macrophytes. The sampling points are depicted by white squares (H1 to H6), and the water flow within the CW with striped arrows. Non-treated water flow discharging to the Lerma gully is depicted with black arrows, and that of treated water with a white arrow.

Figure 2. Evolution of denitrification in the biostimulated microcosms. NO_3^- (circles joined by a continuous line) and NO_2^- (squares joined by a dashed line) measured in (**A**) the batch experiments employing different C sources and (**B**) the experiments testing the effects of temperature and lifespan of the stubble.

Figure 3. NO_3^--O and NO_3^--N isotopic fractionation throughout denitrification in the biostimulated microcosms. Results from the batch experiments testing (**A, B**) different C sources and (**C, D**) the effects of temperature and lifespan of the stubble.

Figure 4. NO_3^- attenuation in the CW before the application of stubble. Black circles depict the sampling campaigns performed at a ~5.5 L/s flow rate (full symbols for the campaign of June 14, 2017 and empty symbols for that of September 5, 2017), and grey circles depict the sampling campaigns performed at a ~2.5 L/s flow rate (September 12, 2017). (**A**) NO_3^- concentration along the CW flow direction, where dashed lines represent the range of NO_3^- concentrations measured at the inlet of the CW throughout the study period. (**B**) Isotopic characterization including the regression line, where the dashed square represents the range of isotopic compositions measured at the inlet of the CW throughout the study period.

Figure 5. NO_3^- attenuation in the CW after the first application of stubble in autumn. (**A**) NO_3^- concentration along the CW, where dashed lines represent the range of NO_3^- concentrations measured at the inlet of the CW throughout the study period. Full symbols depict the sampling campaign conducted on October 2, 2017, and empty symbols depict that conducted on October 10, 2017 (seven and fourteen days after the application of the stubble, respectively). (**B, C**) NO_3^- concentrations monitored at the inlet (black) and outlet (grey) in the days before and after the sampling campaigns, respectively.

Figure 6. NO_3^- attenuation in the CW after the second application of stubble in spring. (**A**) NO_3^- concentrations monitored at the inlet (black) and outlet (grey) of the CW throughout the first days of treatment. (**B)** NO_3^- concentrations along the CW flow direction, for each sampling campaign. Dashed lines represent the range of NO_3^- concentrations measured at the inlet of the CW throughout the study period. The 7 sampling campaigns performed throughout the 100 days after stubble application are represented by shades of grey (from darker to lighter as time progressed), with the last represented by the empty symbols. The campaign performed before application is represented by asterisks.

Figure 7. Denitrification efficiency in the CW determined from the laboratory-obtained ε values. Isotopic values obtained from the samples collected at the CW, including the regression line (black). The three denitrification % lines (grey) presented correspond to the three conditions tested in the laboratory that were closest to the CW conditions throughout the field-scale test.

Figure 8. Dissolved organic C in the CW before and after application of stubble. NPDOC concentration along the CW flow. The 5 sampling campaigns conducted within the 63 days after stubble application are presented in shades of grey, from darkest to lightest as time progressed. The campaign performed before application is represented by asterisks.

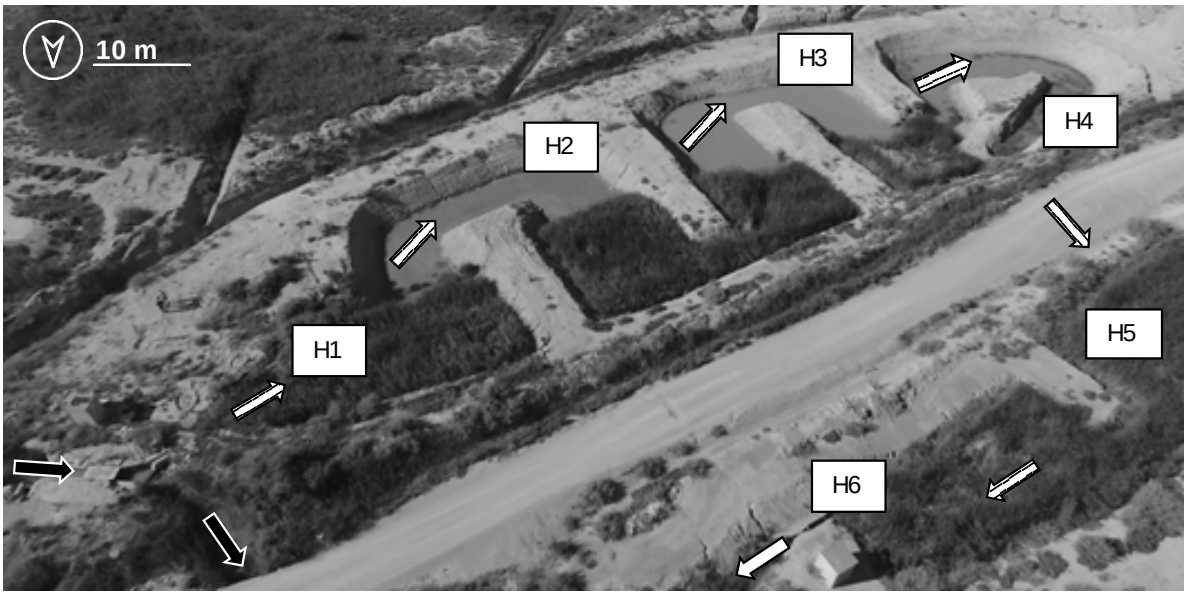
10 m
H1
H2
H3
H4
H5
H6

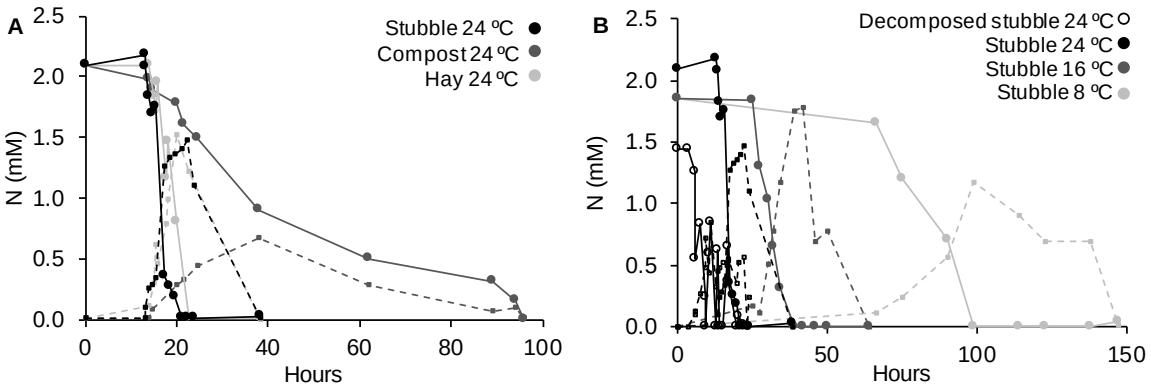
A
B
N (mM)
Hours
Stubble 24 ºC
Compost 24 ºC
Hay 24 ºC
Decomposed stubble 24 ºC
Stubble 24 ºC
Stubble 16 ºC
Stubble 8 ºC

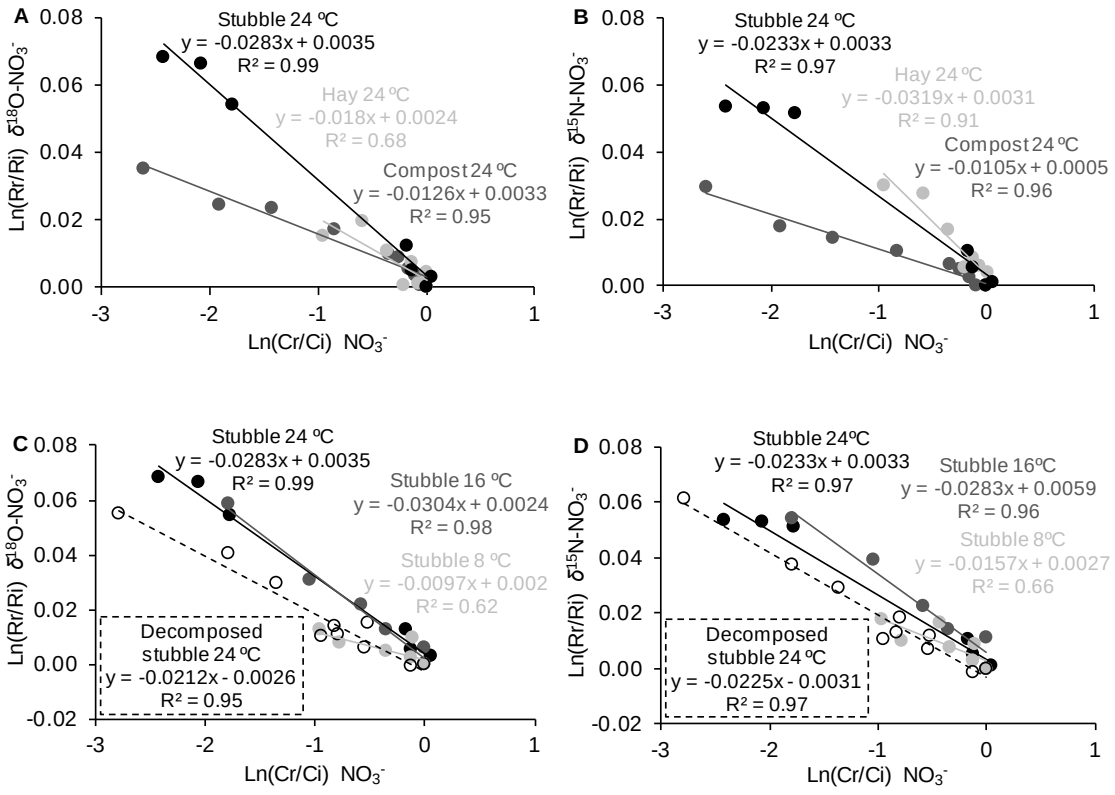
A
Stubble 24 ºC
y = -0.0283x + 0.0035
R² = 0.99
Hay 24 ºC
y = -0.018x + 0.0024
R² = 0.68
Compost 24 ºC
y = -0.0126x + 0.0033
R² = 0.95
Ln(Rr/Ri) δ18O-NO3-
Ln(Cr/Ci) NO3-
B
Stubble 24 ºC
y = -0.0233x + 0.0033
R² = 0.97
Hay 24 ºC
y = -0.0319x + 0.0031
R² = 0.91
Compost 24 ºC
y = -0.0105x + 0.0005
R² = 0.96
Ln(Rr/Ri) δ15N-NO3-
Ln(Cr/Ci) NO3-
C
Stubble 24 ºC
y = -0.0283x + 0.0035
R² = 0.99
Stubble 16 ºC
y = -0.0304x + 0.0024
R² = 0.98
Stubble 8 ºC
y = -0.0097x + 0.002
R² = 0.62
Decomposed stubble 24 ºC
y = -0.0212x - 0.0026
R² = 0.95
Ln(Rr/Ri) δ18O-NO3-
Ln(Cr/Ci) NO3-
D
Stubble 24ºC
y = -0.0233x + 0.0033
R² = 0.97
Stubble 16ºC
y = -0.0283x + 0.0059
R² = 0.96
Stubble 8ºC
y = -0.0157x + 0.0027
R² = 0.66
Decomposed stubble 24 ºC
y = -0.0225x - 0.0031
R² = 0.97
Ln(Rr/Ri) δ15N-NO3-
Ln(Cr/Ci) NO3-

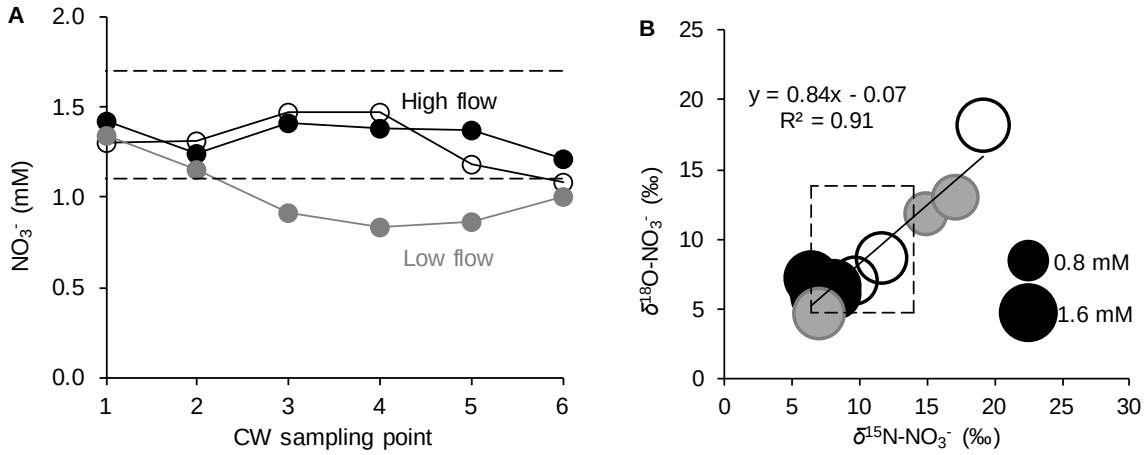
A
2.0
1.5
1.0
0.5
0.0
NO3- (mM)
High flow
Low flow
1
2
3
4
5
6
CW sampling point
B
25
20
15
10
5
0
y = 0.84x - 0.07
R² = 0.91
δ18O-NO3- (‰)
0.8 mM
1.6 mM
0
5
10
15
20
25
30
δ15N-NO3- (‰)

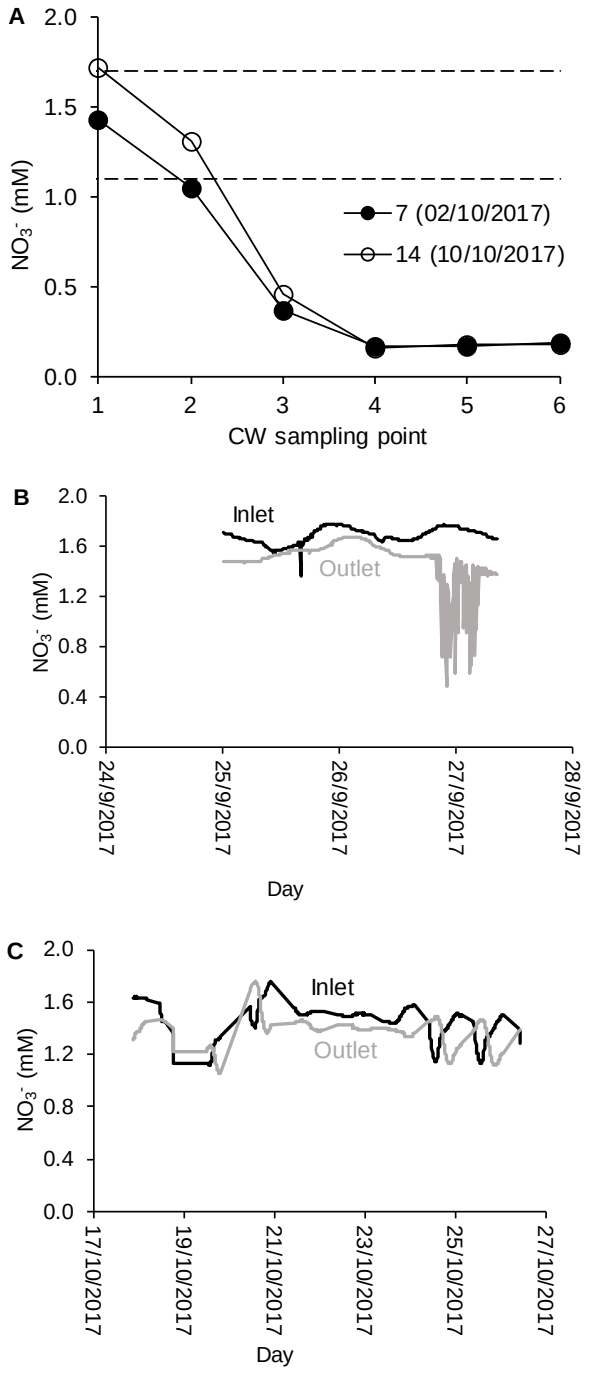
A
2.0
1.5
1.0
0.5
0.0
NO_3^- (mM)
7 (02/10/2017)
14 (10/10/2017)
1
2
3
4
5
6
CW sampling point
B
2.0
1.6
1.2
0.8
0.4
0.0
NO_3^- (mM)
Inlet
Outlet
24/9/2017
25/9/2017
26/9/2017
27/9/2017
28/9/2017
Day
C
2.0
1.6
1.2
0.8
0.4
0.0
NO_3^- (mM)
Inlet
Outlet
17/10/2017
19/10/2017
21/10/2017
23/10/2017
25/10/2017
27/10/2017
Day

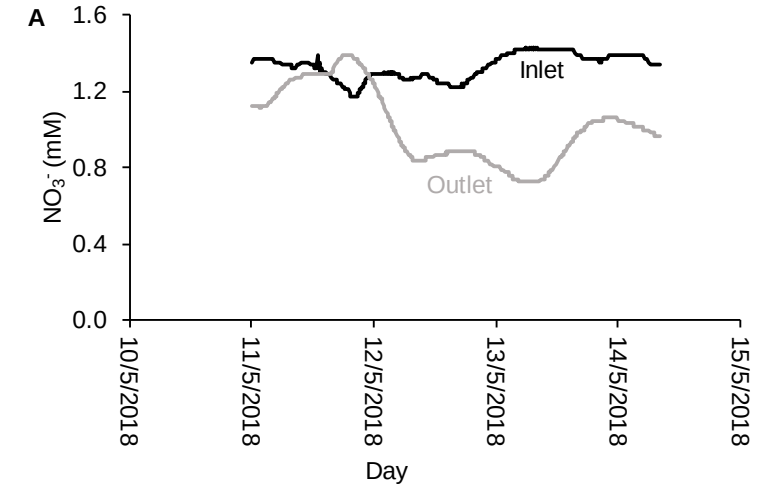
A
1.6
1.2
0.8
0.4
0.0
NO_3^- (mM)
Inlet
Outlet
10/5/2018
11/5/2018
12/5/2018
13/5/2018
14/5/2018
15/5/2018
Day

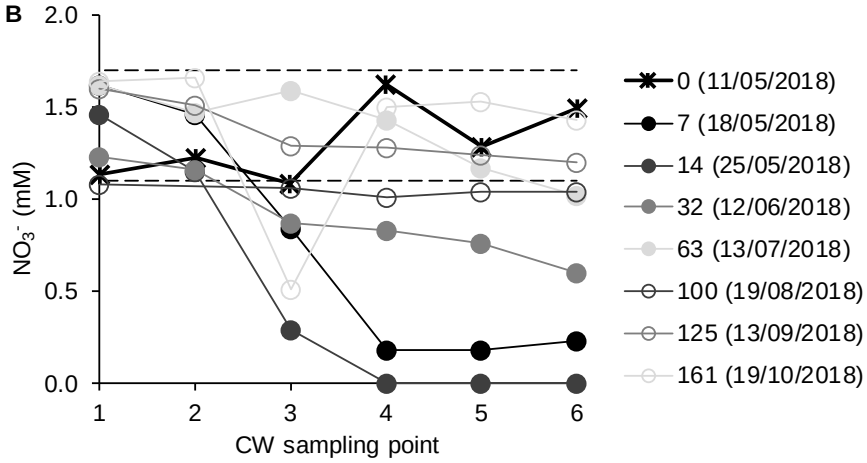
B
2.0
1.5
1.0
0.5
0.0
NO_3^- (mM)
1
2
3
4
5
6
CW sampling point
0 (11/05/2018)
7 (18/05/2018)
14 (25/05/2018)
32 (12/06/2018)
63 (13/07/2018)
100 (19/08/2018)
125 (13/09/2018)
161 (19/10/2018)

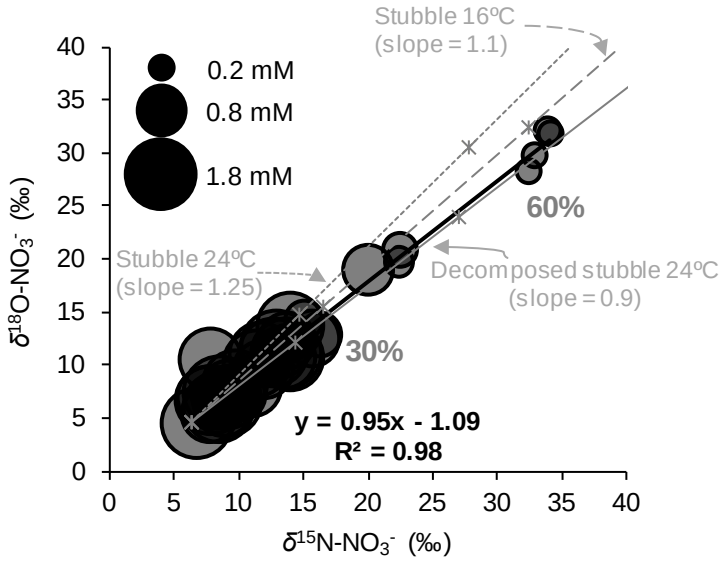
Stubble 16ºC
(slope = 1.1)
0.2 mM
0.8 mM
1.8 mM
60%
Stubble 24ºC
(slope = 1.25)
Decomposed stubble 24ºC
(slope = 0.9)
30%
y = 0.95x - 1.09
R² = 0.98
δ18O-NO3- (‰)
δ15N-NO3- (‰)
0
5
10
15
20
25
30
35
40

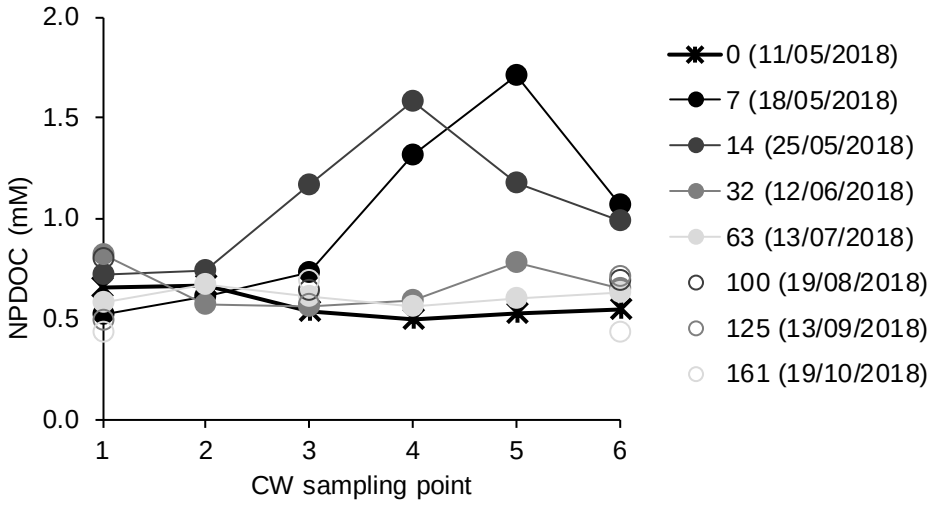
2.0
1.5
1.0
0.5
0.0
NPDOC (mM)
1
2
3
4
5
6
CW sampling point
0 (11/05/2018)
7 (18/05/2018)
14 (25/05/2018)
32 (12/06/2018)
63 (13/07/2018)
100 (19/08/2018)
125 (13/09/2018)
161 (19/10/2018)

Table 1. Series of experiments. Tested conditions and composition of microcosms. DIW = deionized water.

Series	Condition	Code	C source	Material (g)	C (g/L)	Water source (100 mL)	Temperature (ºC)
I	Biostimulated	C-24	Animal compost	0.25	0.8	Wetland	24
	Control	C-24-blank	Animal compost	0.25	0.8	DIW	24
II	Biostimulated	H-24	Wheat hay	1	4.2	Wetland	24
	Control	H-24-blank	Wheat hay	1	4.2	DIW	24
III	Biostimulated	S-24	Corn stubble	1	3.6	Wetland	24
	Control	S-24-blank	Corn stubble	1	3.6	DIW	24
IV	Biostimulated	S-16	Corn stubble	1	3.6	Wetland	16
	Control	S-16-blank	Corn stubble	1	3.6	DIW	16
V	Biostimulated	S-8	Corn stubble	1	3.6	Wetland	8
	Control	S-8-blank	Corn stubble	1	3.6	DIW	8
VI	Biostimulated	DS-24	Decomposed stubble	1	3.6	Wetland	24
	Control	DS-24-blank	Decomposed stubble	1	3.6	DIW	24

Table 2. Sampling campaigns. Sampling dates and operation mode of the CW for all sampling campaigns (six samples each).

Test period	Date	Days since stubble addition	Operation mode	Observations
I	14/06/2017	-	High flow	No external organic C addition
	05/09/2017	-	High flow	
	12/09/2017	-	Low flow	
II	02/10/2017	7	High flow	First organic C source addition on 25/09/2017
	10/10/2017	14		
III	11/05/2018	0	High flow	Second organic C source addition on 11/05/2018
	18/05/2018	7		
	25/05/2018	14		
	12/06/2018	32		
	13/07/2018	63		
	19/08/2018	100		
	13/09/2018	125		
	19/10/2018	161		

Table 3. Waste products composition. C and N concentrations and isotopic composition of the corn stubble, wheat hay, and animal compost employed to promote denitrification.

SOURCE	C (%)	N (%)	δ^{13}C (‰)	δ^{15}N (‰)
Animal compost	32.1	3.1	-25.4	10.8
Wheat hay	40.9	0.4	-27.8	3.0
Corn stubble	36.1	1.0	-13.6	6.7

Table 4. Calculated ε values from the laboratory microcosms. $\varepsilon^{18}O_{NO3/N2}$, $\varepsilon^{15}N_{NO3/N2}$, and $\varepsilon^{15}N_{NO3/N2}/\varepsilon^{18}O_{NO3/N2}$ for each condition tested at laboratory-scale.

EXPERIMENT	$\varepsilon^{18}O_{NO3/N2}$	$\varepsilon^{15}N_{NO3/N2}$	$\varepsilon^{15}N/\varepsilon^{18}O$
Compost 24ºC	-12.6	-10.5	0.8
Hay 24ºC	-18.0	-31.9	1.8
Stubble 24ºC	-28.3	-23.3	0.8
Stubble 16ºC	-30.4	-28.3	0.9
Stubble 8ºC	-9.7	-15.7	1.6
Decomposed stubble 24ºC	-21.2	-22.5	1.1

Supporting Information, section S1: δ^{13}C-DIC results

The δ^{13}C-DIC results provided information about the transformation of organic C from the waste materials to inorganic C (**Equation S1**). These results are presented in Supporting Information **Table S2**. As DIC concentration increased, the initial δ^{13}C-DIC in water of -13.1 ‰ decreased to -15.5 ‰ and -20.0 ‰ in the microcosms containing hay and compost, respectively, but remained unchanged in the stubble experiment (**Figure S2**). The flat trend observed in the experiments with stubble, in contrast to the correlations obtained with the experiments employing hay and compost, was attributed to the intrinsic δ^{13}C-C_{bulk} of each material (**Table 3**). The most significant change in the δ^{13}C-DIC was observed for the experiment involving hay, which presented a lower δ^{13}C-C_{bulk} (-27.8 ‰) compared to that of compost (-25.4‰); stubble did not produce any change because its δ^{13}C-C_{bulk} (-13.6 ‰) is close to the δ^{13}C-DIC of water (-13.1 ‰). Hay and stubble presented a different intrinsic δ^{13}C-C_{bulk} as they are classified as C4 and C3 plants, respectively (Leary, 1988). An isotopic fractionation effect derived from the bacterial C metabolism did not seem to be significant under the tested conditions. These results show that the δ^{13}C-DIC analysis can be applied to assess the efficiency of biostimulation strategies at field-scale when C sources with an intrinsic δ^{13}C-C_{bulk} differing from the δ^{13}C-DIC of water (such as C4 plant materials) are used.

$$5\ CH_2O + 4\ NO_3^- + 4\ H^+ \rightarrow 2\ N_2 + 5\ CO_2 + 7\ H_2O \qquad \textbf{Equation S1}$$

References:

Leary, M.H.O., 1988. Carbon Isotopes in Photosynthesis. Bioscience 38, 328–336.

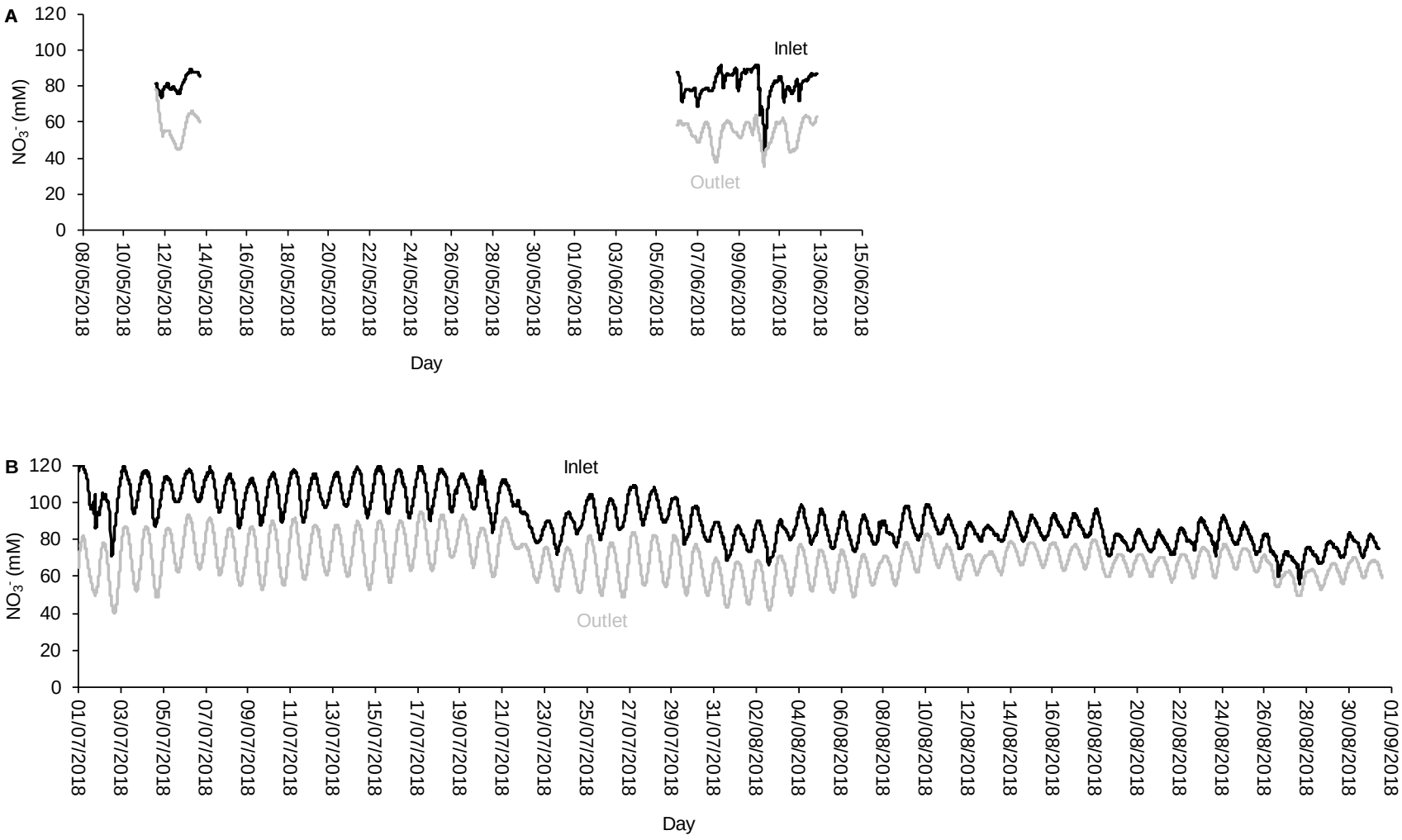
A
120
100
80
60
40
20
0
NO_3^- (mM)
Inlet
Outlet
08/05/2018
10/05/2018
12/05/2018
14/05/2018
16/05/2018
18/05/2018
20/05/2018
22/05/2018
24/05/2018
26/05/2018
28/05/2018
30/05/2018
01/06/2018
03/06/2018
05/06/2018
07/06/2018
09/06/2018
11/06/2018
13/06/2018
15/06/2018
Day
B
120
100
80
60
40
20
0
NO_3^- (mM)
Inlet
Outlet
01/07/2018
03/07/2018
05/07/2018
07/07/2018
09/07/2018
11/07/2018
13/07/2018
15/07/2018
17/07/2018
19/07/2018
21/07/2018
23/07/2018
25/07/2018
27/07/2018
29/07/2018
31/07/2018
02/08/2018
04/08/2018
06/08/2018
08/08/2018
10/08/2018
12/08/2018
14/08/2018
16/08/2018
18/08/2018
20/08/2018
22/08/2018
24/08/2018
26/08/2018
28/08/2018
30/08/2018
01/09/2018
Day

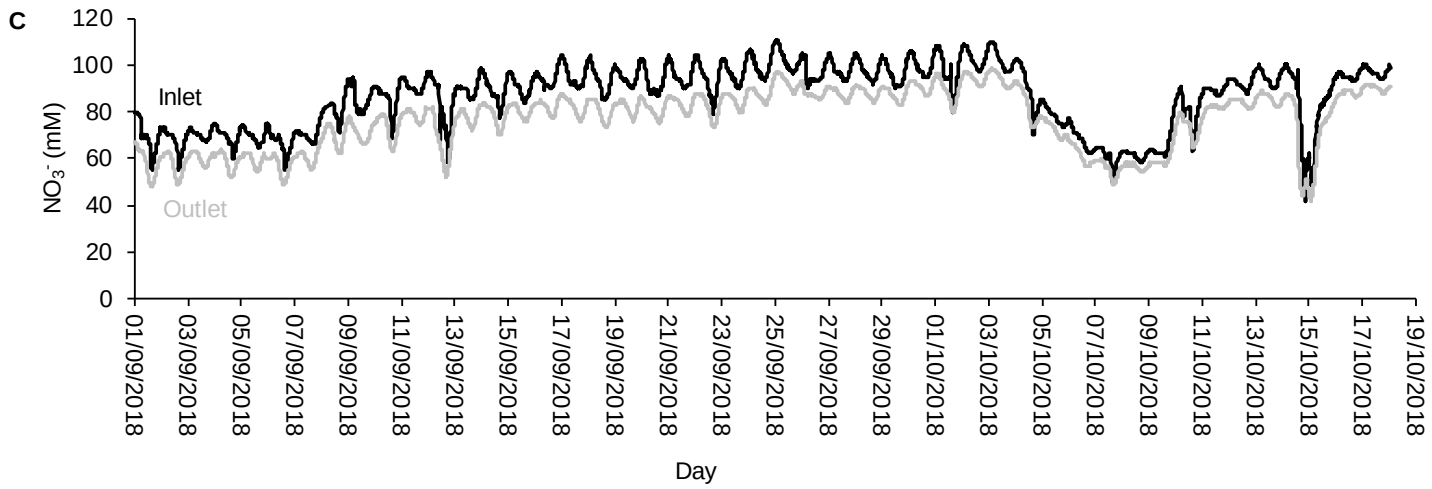

Figure S1. Monitored NO_3^- concentrations at the inlet and outlet of the CW during the third period of the test. The NO_3^- retention time in the CW was considered for the outlet data. (**A**) May-June 2018, (**B**) July-August 2018 and (**C**) September-October 2018. The data between 10/05/2018 and 06/06/2018 and between 13/06/2018 and 01/07/2018 is lacking due to technical issues.

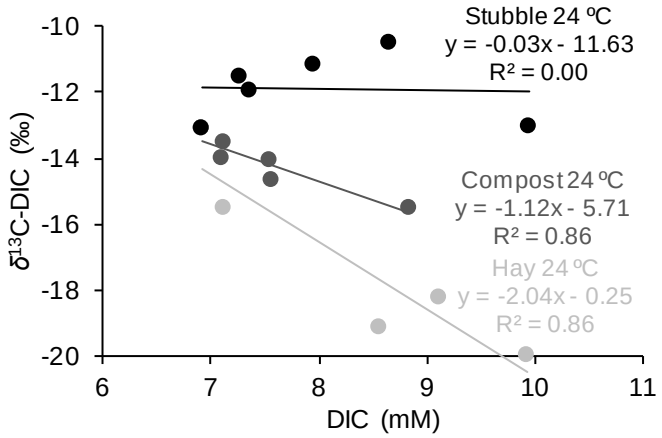

Figure S2. Relationship between δ^{13}C-DIC and DIC concentration throughout denitrification. Correlation between δ^{13}C-DIC and DIC concentration in the samples collected from laboratory batch experiments testing different C sources for the induction of the bacterial NO_3^- reduction.

Table S1. Precipitation and temperature records. Data collected from a meteorological station near the CW (coordinates X = 649168.18 and Y = 4662201.55).

Month	Precipitation (mm)	Average temperature (ºC)	Minimum temperature (ºC)	Maximum temperature (ºC)
June-17	80.2	23.2	13.2	30.2
July-17	46.6	23.6	15.1	28.3
August-17	79.4	23.2	16.5	29.1
September-17	47.2	17.6	12.5	23.3
October-17	11.1	16.0	10.3	20.4
November-17	13.1	8.6	2.5	15.3
December-17	17.3	5.1	0.3	9.4
January-18	64.5	6.8	2.0	12.7
February-18	37.6	4.9	0.9	10.0
March-18	82.8	8.5	3.8	12.3
April-18	173.9	12.8	5.8	16.8
May-18	54.7	15.8	9.6	20.0
June-18	17.3	20.9	15.8	26.2
July-18	44.2	24.6	19.9	28.4
August-18	4.4	23.8	19.1	28.2
September-18	19.7	21.2	15.9	23.9
October-18	0.0	16.3	13.1	18.8

Table S2. Standards for isotopic analysis. International and laboratory (CCiT) standards used for normalization of the results.

Analysis	Standards
$\delta^{15}N\text{-}NO_3^-$	USGS-32, USGS-34, USGS-35 and CCiT-IWS ($\delta^{15}N$ = +16.9 ‰)
$\delta^{18}O\text{-}NO_3^-$	USGS-32, USGS-34, USGS-35 and CCiT-IWS ($\delta^{18}O$ = +28.5 ‰)
$\delta^{15}N\text{-}N_{bulk}$	USGS-40, IAEA-N1, IAEA-NO3, IAEA-N2
$\delta^{13}C\text{-}C_{bulk}$	USGS-40, IAEA-CH7, IAEA-CH6
$\delta^{13}C$-DIC	CCiT-$NaHCO_3$ ($\delta^{13}C$ = -4.4 ‰), CCiT-$NaKHCO_3$ ($\delta^{13}C$ = -18.7 ‰) and CCiT-$KHCO_3$ ($\delta^{13}C$ = +29.2 ‰)
$\delta^{34}S\text{-}SO_4^{2-}$	NBS-127, SO5, SO6 and CCiT-YCEM ($\delta^{34}S$ = +12.8 ‰)
$\delta^{18}O\text{-}SO_4^{2-}$	NBS-127, SO6, USGS-34, CCiT-YCEM ($\delta^{18}O$ = +17.6 ‰) and CCiT-ACID ($\delta^{18}O$ = +13.2 ‰)

Table S3. Batch experiments results. N and C compounds concentration and isotopic composition.

Code	Hour	NO_3^- (mM)	NO_2^- (mM)	NH_4^+ (mM)	N_2O (nmol)	N_2O (%)*	NPDOC (mM)	DIC (mM)	$\delta^{15}N\text{-}NO_3^-$ (‰)	$\delta^{18}O\text{-}NO_3^-$ (‰)	$\delta^{13}C\text{-}DIC$ (‰)
CW water	0.0	2.1	0.0	0.0	n.d.	n.d.	0.5	6.9	6.4	4.9	-13.1
C-24-1	14.0	2.0	0.0	0.1	n.d.	n.d.	10.2	7.1	4.6	5.7	-13.5
C-24-2	14.5	1.9	0.1	0.1	n.d.	n.d.	n.d.	n.d.	6.7	8.5	n.d.
C-24-3	20.0	1.8	0.3	0.1	n.d.	n.d.	9.0	7.1	9.3	10.6	-14.0
C-24-4	21.5	1.6	0.3	0.1	n.d.	n.d.	n.d.	n.d.	11.6	13.8	n.d.
C-24-5	24.5	1.5	0.4	0.1	n.d.	n.d.	10.6	7.5	13.1	15.2	-14.1
C-24-6	38.0	0.9	0.7	0.1	n.d.	n.d.	8.8	7.6	17.0	22.6	-14.7
C-24-7	62.0	0.5	0.3	0.1	n.d.	n.d.	n.d.	n.d.	21.2	28.9	n.d.
C-24-8	89.0	0.3	0.1	n.d.	n.d.	n.d.	5.3	8.8	24.5	30.0	-15.5
C-24-9	94.0	0.2	0.1	n.d.	n.d.	n.d.	n.d.	n.d.	36.4	41.0	n.d.
C-24-10	96.0	0.0	0.0	n.d.	n.d.	n.d.	7.8	n.d.	n.d.	n.d.	n.d.
C-24-blank	188.0	0.0	0.0	n.d.	n.d.	n.d.	14.3	n.d.	n.d.	n.d.	n.d.
H-24-1	13.8	2.1	0.1	0.1	n.d.	n.d.	14.7	n.d.	10.3	9.5	-18.3
H-24-2	15.0	1.8	0.3	0.1	n.d.	n.d.	13.4	9.1	15.2	12.7	-18.3
H-24-3	15.5	1.7	0.6	n.d.	n.d.	n.d.	n.d.	n.d.	12.3	5.8	n.d.
H-24-4	15.8	1.9	0.5	n.d.	n.d.	n.d.	n.d.	n.d.	12.4	6.3	n.d.
H-24-5	17.8	1.2	0.8	0.0	n.d.	n.d.	11.8	n.d.	34.5	25.1	-17.7
H-24-6	18.0	1.5	1.0	n.d.	n.d.	n.d.	n.d.	n.d.	23.3	15.9	n.d.
H-24-7	20.0	0.8	1.5	n.d.	n.d.	n.d.	n.d.	n.d.	37.0	20.7	n.d.
H-24-8	22.5	0.0	1.2	0.0	n.d.	n.d.	12.5	8.6	n.d.	n.d.	-19.2
H-24-9	38.5	0.0	0.0	0.2	n.d.	n.d.	14.7	9.9	n.d.	n.d.	-20.0
H-24-blank-1	4.0	0.1	0.0	0.0	n.d.	n.d.	n.d.	n.d.	n.d.	n.d.	n.d.
H-24-blank-2	38.5	0.0	0.0	n.d.	n.d.	n.d.	16.9	1.8	n.d.	n.d.	n.d.
S-24-1	13.0	2.2	0.0	0.2	n.d.	n.d.	14.7	9.9	7.8	8.0	-13.0
S-24-2	13.3	2.1	0.1	n.d.	n.d.	n.d.	n.d.	n.d.	n.d.	n.d.	-11.4
S-24-3	14.0	1.8	0.3	n.d.	n.d.	n.d.	15.7	7.3	11.9	10.3	-11.6
S-24-4	14.8	1.7	0.3	n.d.	n.d.	n.d.	n.d.	n.d.	n.d.	n.d.	n.d.
S-24-5	15.5	1.8	0.3	0.3	n.d.	n.d.	18.2	7.4	17.2	17.5	-12.0
S-24-6	17.5	0.3	1.3	n.d.	n.d.	n.d.	13.2	n.d.	59.4	60.8	n.d.
S-24-7	18.5	0.3	1.3	0.1	n.d.	n.d.	n.d.	n.d.	61.1	73.8	n.d.
S-24-8	19.5	0.2	1.4	n.d.	n.d.	n.d.	n.d.	n.d.	62.0	76.1	n.d.
S-24-9	21.0	0.0	1.4	0.1	n.d.	n.d.	n.d.	n.d.	n.d.	n.d.	n.d.
S-24-10	22.3	0.0	1.5	n.d.	n.d.	n.d.	15.9	8.0	n.d.	n.d.	-11.2
S-24-11	23.8	0.0	1.1	n.d.	n.d.	n.d.	n.d.	n.d.	n.d.	n.d.	n.d.
S-24-12	38.5	0.0	0.0	1.0	n.d.	n.d.	18.5	8.7	n.d.	n.d.	-10.5
S-24-blank-1	38.5	0.1	0.0	0.0	n.d.	n.d.	27.3	n.d.	n.d.	n.d.	n.d.
CW water	0.0	1.9	0.0	n.d.	n.d.	n.d.	n.d.	n.d.	5.9	8.0	n.d.
S-16-1	25.0	1.8	0.2	n.d.	0.8	0.001	n.d.	n.d.	17.4	14.3	n.d.
S-16-2	27.0	1.3	0.1	n.d.	0.6	0.001	n.d.	n.d.	20.5	20.5	n.d.

S-16-3	30.0	1.0	0.5	n.d.	n.d.	n.d.	n.d.	n.d.	28.7	29.8	n.d.
S-16-4	32.0	0.6	0.8	n.d.	2.5	0.002	n.d.	n.d.	46.2	39.7	n.d.
S-16-5	34.0	0.3	1.2	n.d.	n.d.	n.d.	n.d.	n.d.	62.1	68.6	n.d.
S-16-6	39.0	0.0	1.7	n.d.	8.7	0.009	n.d.	n.d.	n.d.	n.d.	n.d.
S-16-7	42.0	0.0	1.8	n.d.	1.9	0.002	n.d.	n.d.	n.d.	n.d.	n.d.
S-16-8	46.0	0.0	0.7	n.d.	0.4	0.000	n.d.	n.d.	n.d.	n.d.	n.d.
S-16-9	50.0	0.0	0.8	n.d.	1.1	0.001	n.d.	n.d.	n.d.	n.d.	n.d.
S-16-10	64.0	0.0	0.0	n.d.	n.d.	n.d.	n.d.	n.d.	n.d.	n.d.	n.d.
S-8'-1	66.0	1.6	0.0	n.d.	n.d.	n.d.	n.d.	n.d.	9.0	10.1	n.d.
S-8'-2	99.0	1.3	0.3	n.d.	n.d.	n.d.	n.d.	n.d.	13.6	13.0	n.d.
S-8'-3	114.0	0.9	0.3	n.d.	n.d.	n.d.	n.d.	n.d.	16.4	15.7	n.d.
S-8-1	66.0	1.7	0.1	n.d.	1.5	0.001	n.d.	n.d.	15.0	17.4	n.d.
S-8-2	75.0	1.2	0.2	n.d.	1.8	0.002	n.d.	n.d.	22.9	n.d.	n.d.
S-8-3	90.0	0.7	0.6	n.d.	2.0	0.002	n.d.	n.d.	24.3	20.6	n.d.
S-8-4	99.0	0.0	1.2	n.d.	5.1	0.005	n.d.	n.d.	n.d.	n.d.	n.d.
S-8-5	114.0	0.0	0.9	n.d.	2.8	0.003	n.d.	n.d.	n.d.	n.d.	n.d.
S-8-6	123.0	0.0	0.7	n.d.	0.0	0.000	n.d.	n.d.	n.d.	n.d.	n.d.
S-8-7	138.0	0.0	0.7	n.d.	3.4	0.003	n.d.	n.d.	n.d.	n.d.	n.d.
S-8-8	147.0	0.0	0.0	n.d.	0.6	0.001	n.d.	n.d.	n.d.	n.d.	n.d.
CW water	0.0	1.4	0.0	n.d.	n.d.	n.d.	0.5	n.d.	14.5	13.4	n.d.
DS-24-1	3.5	1.4	0.0	n.d.	n.d.	n.d.	n.d.	n.d.	n.d.	n.d.	n.d.
DS-24-2	5.5	1.3	0.1	0.1	n.d.	n.d.	2.2	n.d.	13.5	12.8	n.d.
DS-24-3	6.0	0.6	0.1	0.0	2.9	0.003	1.7	n.d.	25.2	23.9	n.d.
DS-24-4	7.5	0.8	0.3	n.d.	n.d.	n.d.	n.d.	n.d.	21.5	19.3	n.d.
DS-24-5	9.0	0.2	0.5	n.d.	1.6	0.002	1.9	n.d.	53.1	55.0	n.d.
DS-24-6	9.5	0.0	0.7	1.3	n.d.	n.d.	2.5	n.d.	n.d.	n.d.	n.d.
DS-24-7	10.5	0.6	0.4	n.d.	n.d.	n.d.	n.d.	n.d.	n.d.	n.d.	n.d.
DS-24-8	11.0	0.9	0.8	n.d.	5.4	0.005	n.d.	n.d.	26.7	28.6	n.d.
DS-24-9	12.5	0.0	0.3	n.d.	n.d.	n.d.	n.d.	n.d.	n.d.	n.d.	n.d.
DS-24-10	13.3	0.6	0.5	1.0	n.d.	n.d.	n.d.	n.d.	28.1	27.6	n.d.
DS-24-11	14.0	0.0	0.5	n.d.	n.d.	n.d.	1.7	n.d.	n.d.	n.d.	n.d.
DS-24-12	15.0	0.0	0.5	n.d.	n.d.	n.d.	n.d.	n.d.	n.d.	n.d.	n.d.
DS-24-13	17.0	0.6	0.5	n.d.	15.1	0.015	n.d.	n.d.	33.3	24.2	n.d.
DS-24-14	17.0	0.4	0.6	0.9	11.7	0.012	n.d.	n.d.	44.3	43.6	n.d.
DS-24-15	20.0	0.0	0.4	0.3	n.d.	n.d.	n.d.	n.d.	n.d.	n.d.	n.d.
DS-24-16	20.3	0.1	0.5	n.d.	12.7	0.013	n.d.	n.d.	78.5	70.7	n.d.
DS-24-17	22.0	0.0	0.6	n.d.	n.d.	n.d.	n.d.	n.d.	n.d.	n.d.	n.d.
DS-24-18	23.0	0.0	0.0	0.5	n.d.	n.d.	8.8	n.d.	n.d.	n.d.	n.d.
DS-24-19	24.0	0.0	0.2	n.d.	n.d.	n.d.	1.7	n.d.	n.d.	n.d.	n.d.

* % of initial NO_3^-–N found as N_2O-N

n.d. = non determined

NH_4^+ in the DS-24 experiment was analyzed by ion selective electrode while in the others by spectrophotometry

Table S4. ICP data. Major cations and trace elements concentration measured in the samples from the laboratory experiments (semiquantitative).

Code	Hour	Na	S	Ca	Mg	K	Si	Sr	P	B	Li	Mn	Zn	Cu	Fe	Ba	V	Co	Tl	Cd	Cr
CW water	0.0	326.8	146.3	130.7	99.3	6.2	10.9	4.2	-	0.35	0.12	-	-	0.08	0.01	0.06	0.06	0.01	0.14	-	0.01
C-24-1	14.0	345.0	163.0	125.8	103.4	65.4	11.4	3.9	1.4	0.42	0.13	0.05	0.09	0.04	0.10	0.05	0.07	-	-	-	-
C-24-2	14.5	334.6	151.1	125.4	101.2	43.3	11.1	3.9	0.8	0.39	0.13	0.05	0.06	0.04	0.07	0.05	0.07	0.01	-	-	-
C-24-3	20.0	321.8	151.8	124.0	100.4	58.2	10.9	3.8	1.0	0.40	0.12	0.06	0.07	0.03	0.08	0.05	0.07	-	0.15	-	-
C-24-5	24.5	328.7	160.1	123.2	102.8	68.7	11.3	3.8	1.2	0.42	0.13	0.08	0.11	0.04	0.11	0.05	0.07	-	-	-	-
C-24-6	38.0	325.2	152.3	123.1	104.6	51.6	11.4	3.6	1.4	0.41	0.13	0.11	0.11	0.04	0.12	0.04	0.07	-	-	-	-
C-24-8	89.0	334.2	151.7	125.6	104.5	41.5	12.1	3.6	1.4	0.40	0.13	0.12	0.05	0.05	0.07	0.04	0.07	-	-	0.01	-
H-24-1	13.8	360.3	168.3	139.4	102.3	160.1	22.8	4.3	0.6	0.38	0.13	0.04	0.04	0.03	0.02	0.11	0.07	0.02	-	0.01	-
H-24-2	15.0	362.0	165.3	139.5	105.0	130.8	22.2	4.2	2.3	0.38	0.13	0.05	0.04	0.03	0.02	0.24	0.06	-	-	-	-
H-24-5	17.8	371.4	170.9	141.4	103.0	142.1	22.1	4.3	-	0.38	0.13	0.06	0.05	0.03	0.01	0.11	0.06	-	-	-	-
H-24-8	22.5	365.1	169.0	140.9	103.4	180.9	25.1	4.3	-	0.37	0.13	0.06	0.06	0.03	0.02	0.16	0.07	0.01	-	-	-
H-24-9	38.5	355.7	164.3	140.4	104.1	167.2	31.2	4.4	0.8	0.37	0.13	0.04	0.06	0.03	0.01	0.13	0.06	-	-	-	-
S-24-1	13.0	318.9	155.5	136.2	108.1	130.8	13.4	4.0	1.2	0.48	0.12	0.10	0.09	0.07	0.06	0.08	0.07	-	-	-	-
S-24-2	13.3	324.5	146.8	128.6	101.5	75.5	13.6	3.8	1.6	0.36	0.12	0.11	0.05	0.05	0.04	0.07	0.06	0.01	-	-	-
S-24-3	14.0	325.3	148.8	126.4	101.4	118.2	13.0	3.7	2.2	0.38	0.12	0.13	0.03	0.04	0.04	0.07	0.06	-	0.15	-	-
S-24-5	15.5	329.9	151.8	130.2	103.2	78.9	14.4	3.8	1.4	0.39	0.12	0.17	0.03	0.04	0.04	0.08	0.06	-	-	-	-
S-24-10	22.3	318.4	149.4	130.9	104.5	108.7	13.9	3.8	0.8	0.39	0.13	0.12	0.04	0.05	0.04	0.12	0.07	-	-	-	-
S-24-12	38.5	329.2	150.0	139.0	109.9	99.5	14.4	4.0	1.1	0.39	0.13	0.16	0.04	0.06	0.05	0.10	0.07	0.03	-	-	0.01

All data is expressed as ppm. Hyphen = below detection limit. The Al, As, Be, Mo, Ni, Pb, Sb, Se and Ti were below detection limit in all analyzed samples.

Table S5. CW test results. Chemical and isotopic characterization of the samples collected in the CW previous and after the implementation of the bioremediation strategy.

Date	Point	NO_2^- (mM)	NO_3^- (mM)	NH_4^+ (mM)	DIC (mM)	NPDOC (mM)	SO_4^{2-} (mM)	$\delta^{13}C$-DIC (‰)	$\delta^{15}N$-NO_3^- (‰)	$\delta^{18}O$-NO_3^- (‰)	$\delta^{34}S$-SO_4^{2-} (‰)	$\delta^{18}O$-SO_4^{2-} (‰)	NO_3^- attenuation		
													%[1]	%[2]	kg/d
14/06/17	H1	0.0	1.4	n.d.	7.1	n.d.	n.d.	n.d.	6.4	7.2	0.8	12.5	n.d.	n.d.	n.d.
	H2	0.0	1.2	n.d.	6.9	n.d.	n.d.	n.d.	6.8	5.9	n.d.	n.d.	n.d.	n.d.	n.d.
	H3	0.0	1.4	n.d.	6.8	n.d.	n.d.	n.d.	6.8	6.5	1.8	12.7	n.d.	n.d.	n.d.
	H4	0.0	1.4	n.d.	n.d.	n.d.	n.d.	n.d.	8.1	6.7	n.d.	n.d.	n.d.	n.d.	n.d.
	H5	0.0	1.4	n.d.	6.9	n.d.	n.d.	n.d.	7.5	6.6	n.d.	n.d.	n.d.	n.d.	n.d.
	H6	0.0	1.2	n.d.	7.0	n.d.	n.d.	n.d.	8.3	6.1	2.5	12.4	n.d.	n.d.	n.d.
05/09/17	H1	0.0	1.3	0.0	7.5	0.6	n.d.	-12.9	11.6	8.7	n.d.	n.d.	n.d.	n.d.	n.d.
	H2	0.0	1.3	n.d.	7.3	0.5	n.d.	-12.7	n.d.	n.d.	n.d.	n.d.	n.d.	n.d.	n.d.
	H3	0.0	1.5	0.0	7.4	0.4	n.d.	-12.7	19.2	18.2	n.d.	n.d.	n.d.	n.d.	n.d.
	H4	0.0	1.5	n.d.	7.5	0.6	n.d.	-12.2	n.d.	n.d.	n.d.	n.d.	n.d.	n.d.	n.d.
	H5	0.0	1.2	n.d.	7.3	0.5	n.d.	-12.8	n.d.	n.d.	n.d.	n.d.	n.d.	n.d.	n.d.
	H6	0.0	1.1	0.0	7.3	0.5	n.d.	-12.4	9.6	7.1	n.d.	n.d.	n.d.	n.d.	n.d.
12/09/17	H1	0.0	1.3	0.0	7.1	0.4	n.d.	-12.4	7.0	4.7	3.4	13.5	n.d.	n.d.	n.d.
	H2	0.0	1.2	n.d.	7.5	0.5	n.d.	-12.8	n.d.	n.d.	n.d.	n.d.	n.d.	n.d.	n.d.
	H3	0.0	0.9	0.0	7.1	0.5	n.d.	-12.5	14.9	11.8	3.6	13.8	n.d.	n.d.	n.d.
	H4	0.0	0.8	n.d.	6.5	0.6	n.d.	-12.1	n.d.	n.d.	n.d.	n.d.	n.d.	n.d.	n.d.
	H5	0.0	0.9	n.d.	6.4	0.6	n.d.	-11.8	n.d.	n.d.	n.d.	n.d.	n.d.	n.d.	n.d.
	H6	0.0	1.0	0.0	6.6	0.5	n.d.	-12.0	17.1	13.0	3.1	13.1	n.d.	n.d.	n.d.
02/10/17	H1	0.0	1.4	0.0	7.0	0.4	4.2	-12.7	9.7	8.4	n.d.	n.d.	0.0	0.0	n.d.
	H2	0.1	1.1	n.d.	7.5	0.8	4.2	-11.8	13.7	12.4	n.d.	n.d.	26.5	16.8	n.d.
	H3	0.1	0.4	0.0	8.2	1.3	3.7	-12.1	22.4	20.9	n.d.	n.d.	73.8	43.9	n.d.
	H4	0.2	0.2	n.d.	8.9	1.9	4.5	-11.7	n.d.	n.d.	n.d.	n.d.	87.8	n.d.	n.d.
	H5	0.2	0.2	n.d.	9.1	1.3	4.7	-12.0	n.d.	n.d.	n.d.	n.d.	87.8	n.d.	n.d.

	H6	0.2	0.2	0.0	9.1	2.3	4.4	-13.1	32.9	29.9	n.d.	n.d.	86.3	64.0	78.4
10/10/17	H1	0.0	1.7	0.0	n.d.	0.4	3.7	-12.6	8.5	7.4	3.9	13.9	0.0	0.0	n.d.
	H2	0.0	1.3	n.d.	7.6	0.6	3.7	-12.0	11.7	11.0	n.d.	n.d.	23.8	14.2	n.d.
	H3	0.1	0.5	0.0	8.1	0.9	3.0	-11.4	15.1	14.4	4.3	12.9	72.9	26.6	n.d.
	H4	0.1	0.2	n.d.	8.7	1.6	3.0	-11.1	n.d.	n.d.	n.d.	n.d.	90.7	n.d.	n.d.
	H5	0.1	0.2	n.d.	8.8	1.1	3.9	-11.5	n.d.	n.d.	n.d.	n.d.	89.1	n.d.	n.d.
	H6	0.1	0.2	0.0	n.d.	1.1	3.9	-11.5	34.1	31.9	4.4	12.6	89.5	68.1	100.3
11/05/18	H1	0.0	1.1	0.0	6.9	0.7	3.9	n.d.	11.1	8.0	4.2	12.4	n.d.	n.d.	n.d.
	H2	0.0	1.2	n.d.	7.0	0.7	4.3	n.d.	n.d.	n.d.	n.d.	n.d.	n.d.	n.d.	n.d.
	H3	0.0	1.1	0.0	6.8	0.5	4.2	n.d.	n.d.	n.d.	4.3	12.1	n.d.	n.d.	n.d.
	H4	0.0	1.6	n.d.	0.0	0.5	5.2	n.d.	13.7	11.1	n.d.	n.d.	n.d.	n.d.	n.d.
	H5	0.0	1.3	n.d.	6.9	0.5	5.4	n.d.	13.5	10.7	4.4	12.1	n.d.	n.d.	n.d.
	H6	0.0	1.5	0.0	6.9	0.5	5.4	n.d.	12.7	11.2	n.d.	n.d.	n.d.	n.d.	n.d.
18/05/18	H1	0.0	1.6	0.0	7.1	0.5	5.7	n.d.	12.9	11.9	3.9	12.2	0.0	0.0	n.d.
	H2	0.0	1.5	0.0	7.2	0.6	5.6	n.d.	13.9	10.7	n.d.	n.d.	9.9	0.0	n.d.
	H3	0.1	0.8	0.1	0.0	0.7	5.7	n.d.	20.1	19.0	3.7	12.1	48.0	27.8	n.d.
	H4	0.1	0.2	0.3	8.0	1.3	5.5	n.d.	n.d.	n.d.	n.d.	n.d.	88.8	n.d.	n.d.
	H5	0.1	0.2	0.3	7.9	1.7	5.7	n.d.	32.4	28.2	n.d.	n.d.	88.8	55.8	n.d.
	H6	0.1	0.2	0.1	7.9	1.1	5.5	n.d.	33.9	32.1	3.9	12.2	85.7	61.0	84.5
25/05/18	H1	0.0	1.5	0.0	7.2	0.7	5.8	n.d.	14.0	13.8	3.6	12.4	0.0	0.0	n.d.
	H2	0.0	1.2	0.1	7.5	0.7	5.7	n.d.	11.9	9.5	n.d.	n.d.	21.3	0.0	n.d.
	H3	0.1	0.3	0.0	8.1	1.2	5.3	n.d.	22.4	19.7	4.2	11.8	79.9	27.7	28.1
	H4	0.0	0.0	0.1	9.4	1.6	4.4	n.d.	n.d.	n.d.	n.d.	n.d.	100.0	n.d.	n.d.
	H5	0.1	0.0	0.1	8.1	1.2	5.4	n.d.	n.d.	n.d.	3.9	11.8	100.0	n.d.	n.d.
	H6	0.1	0.0	0.0	8.3	1.0	5.2	n.d.	n.d.	n.d.	n.d.	n.d.	100.0	n.d.	n.d.
12/06/18	H1	0.0	1.2	0.0	0.0	0.8	4.2	n.d.	9.2	7.0	3.9	12.6	0.0	0.0	n.d.
	H2	0.0	1.2	0.0	7.4	0.6	4.3	n.d.	n.d.	n.d.	n.d.	n.d.	5.9	n.d.	n.d.
	H3	0.0	0.9	n.d.	7.3	0.6	4.2	n.d.	10.0	7.1	3.8	12.5	29.4	2.1	n.d.
	H4	0.0	0.8	0.0	0.0	0.6	4.2	n.d.	n.d.	n.d.	n.d.	n.d.	32.1	n.d.	n.d.

	H5	0.1	0.8	n.d.	0.0	0.8	4.3	n.d.	n.d.	n.d.	n.d.	n.d.	37.7	n.d.	n.d.
	H6	0.1	0.6	0.0	7.6	0.7	4.3	n.d.	16.3	12.9	3.9	12.4	51.2	25.8	27.1
13/07/18	H1	0.0	1.6	0.0	6.9	0.6	3.5	n.d.	8.4	6.1	n.d.	n.d.	0.0	0.0	n.d.
	H2	0.0	1.5	0.0	6.7	0.7	3.6	n.d.	n.d.	n.d.	n.d.	n.d.	9.7	n.d.	n.d.
	H3	0.0	1.6	0.0	7.1	0.6	3.4	n.d.	9.2	6.6	n.d.	n.d.	2.2	n.d.	n.d.
	H4	0.0	1.4	0.0	0.0	0.6	3.3	n.d.	n.d.	n.d.	n.d.	n.d.	12.0	n.d.	n.d.
	H5	0.1	1.2	n.d.	7.6	0.6	3.3	n.d.	n.d.	n.d.	n.d.	n.d.	27.8	n.d.	n.d.
	H6	0.1	1.0	0.0	0.0	0.6	3.3	n.d.	15.7	12.6	n.d.	n.d.	36.8	26.9	37.4
19/08/18	H1	0.0	1.1	n.d.	0.0	0.8	2.2	n.d.	7.7	5.4	4.7	12.2	0.0	0.0	n.d.
	H3	0.0	1.1	n.d.	0.0	0.6	2.2	n.d.	n.d.	n.d.	4.6	11.9	1.8	n.d.	n.d.
	H4	0.0	1.0	n.d.	7.8	n.d.	2.2	n.d.	n.d.	n.d.	n.d.	n.d.	7.0	n.d.	n.d.
	H5	0.0	1.0	n.d.	n.d.	n.d.	2.1	n.d.	n.d.	n.d.	n.d.	n.d.	4.5	n.d.	n.d.
	H6	0.0	1.0	n.d.	n.d.	0.7	2.1	n.d.	8.8	5.8	4.0	11.8	4.1	3.3	3.1
13/09/18	H1	0.0	1.6	n.d.	n.d.	0.5	2.4	n.d.	7.8	6.7	n.d.	n.d.	0.0	0.0	n.d.
	H2	0.0	1.5	n.d.	n.d.	n.d.	2.5	n.d.	n.d.	n.d.	n.d.	n.d.	5.7	n.d.	n.d.
	H3	0.0	1.3	n.d.	n.d.	0.6	2.5	n.d.	7.6	7.0	n.d.	n.d.	19.0	0.3	n.d.
	H4	0.0	1.3	n.d.	n.d.	n.d.	2.5	n.d.	7.9	10.6	n.d.	n.d.	19.7	8.5	n.d.
	H5	0.0	1.2	n.d.	n.d.	n.d.	2.5	n.d.	n.d.	n.d.	n.d.	n.d.	22.3	n.d.	n.d.
	H6	0.0	1.2	n.d.	n.d.	0.7	2.5	n.d.	9.2	7.6	n.d.	n.d.	24.7	5.0	6.9
19/10/18	H1	0.0	1.6	n.d.	n.d.	0.4	2.6	n.d.	6.7	4.5	n.d.	n.d.	0.0	0.0	n.d.
	H2	0.0	1.7	n.d.	n.d.	n.d.	2.5	n.d.	n.d.	n.d.	n.d.	n.d.	-1.4	n.d.	n.d.
	H3	0.0	0.5	n.d.	n.d.	0.7	2.6	n.d.	7.8	7.1	n.d.	n.d.	68.6	8.3	n.d.
	H4	0.0	1.5	n.d.	n.d.	n.d.	2.6	n.d.	n.d.	n.d.	n.d.	n.d.	8.7	n.d.	n.d.
	H5	0.0	1.5	n.d.	n.d.	n.d.	2.6	n.d.	n.d.	n.d.	n.d.	n.d.	6.6	n.d.	n.d.
	H6	0.0	1.4	n.d.	n.d.	0.4	2.6	n.d.	11.4	10.1	n.d.	n.d.	12.6	21.0	29.4

X^1 is calculated from concentration data while X^2 is calculated from isotopic data

n.d. = non determined

NH_4^+ in the 2017 campaigns was analyzed by ion chromatography while in the 2018 campaigns by ion selective electrode